



# Fire-Resistant and Fragment Penetration-Resistant Blankets for the Protection of Stored Ammunition

Wai K. Chin  
Thomas J. Mulkern  
Archibald Tewarson

ARL-TR-2285

SEPTEMBER 2000

# Fire-Resistant and Fragment Penetration-Resistant Blankets for the Protection of Stored Ammunition

Wai K. Chin  
Thomas J. Mulkern  
Weapons & Materials Research Directorate, ARL

Archibald Tewarson  
Factory Mutual Research Corporation

---

Approved for public release; distribution is unlimited.

---

---

## Abstract

---

Large quantities of munitions stored in the open are vulnerable to a host of initiation threats, both inadvertent and intentional in nature. An experimental flame- and fragment-resistant blanket was developed to protect such munitions and prevent sympathetic reactions when the blanket is used in concert with earthen barricades. The blanket, which consists of aramid and ceramic fibers, passed several rigorous tests in both the laboratory and in the field. The ballistic performance of the blanket offered protection from 300-g and 454-g fragments traveling at velocities of 140 m/s and 60 m/s, respectively. The blanket also provided flame protection from high temperature gas jets, as well as burning JA2 and M30 propellant, when the temperatures exceeded 1200° C for 10 seconds.

This final report combines the research efforts of the fragment penetration study and the flame and heat blocking with fire blankets for munition protection study: U.S. Army Research Laboratory (ARL) technical report, "Fire Blanket for Munition Protection: Flame- and Heat-Blocking Properties of Advanced Materials," to be published by ARL, Aberdeen Proving Ground, Maryland.

## ACKNOWLEDGMENTS

The authors would like to thank Mr. Duane Scarborough and Mr. Robert Rossi of the U.S. Army Defense Ammunition Logistics Activity for funding this research program. We would also like to thank Mr. Vincent Boyle, Dr. Robert Frey, Dr. John Starkenberg, Dr. Warren Hillstrom, Mr. Anthony Canami, Mr. Thomas Adkins, Ms. Dawnn Saunders, and Mr. Gould Gibbons of the Explosive Technology Branch, Weapons and Materials Research Directorate, U.S. Army Research Laboratory, for the use of the experimental facilities and the coordination of the plans.

INTENTIONALLY LEFT BLANK

---

## Contents

---

<b>1.</b>	<b>Introduction and Background</b> . . . . .	<b>1</b>
<b>2.</b>	<b>Experimental</b> . . . . .	<b>6</b>
2.1	Fibers/Fabrics . . . . .	6
2.2	MST Blanket Specimens . . . . .	6
2.3	Flammability . . . . .	7
2.4	Flame Penetration Experiments . . . . .	7
2.5	Heat Penetration Experiments . . . . .	8
2.6	Determination of Exposure Conditions . . . . .	12
2.7	Resistance to Fragment Penetration . . . . .	17
<b>3.</b>	<b>Results and Discussion</b> . . . . .	<b>22</b>
3.1	Flame Penetration Experiments . . . . .	22
3.2	Heat Penetration Experiments . . . . .	25
3.3	Ballistics and Arena Experiments . . . . .	36
3.4	Blanket Design Considerations . . . . .	52
<b>4.</b>	<b>Conclusions</b> . . . . .	<b>53</b>
4.1	Flammability . . . . .	53
4.2	Phase 1 Ballistics . . . . .	55
4.3	Phase 2 Ballistics . . . . .	55
4.4	Sub-Scale Arena Experiments . . . . .	56
4.5	Issues and Concerns . . . . .	56
	<b>References</b> . . . . .	<b>57</b>
	<b>Distribution List</b> . . . . .	<b>59</b>
	<b>Report Documentation Page</b> . . . . .	<b>61</b>
	<b>Figures</b>	
1.	Heat Penetration Apparatus Use in the Experiments for Sample MST Blankets . . . . .	10
2.	Measured Radiant Heat Flux at the Sample Surface Versus Distance Between the Surface and the Radiant Heater in the Heat Penetration Apparatus . . . . .	11
3.	Arrangement of the Sample MST Blanket With Three Layers of Kevlar Fabric at the Back of the Sample MST Blanket on the Horizontal Platform of the Heat Penetration Apparatus . . . . .	11
4.	Average Front and Back Surface Temperatures Above Ambient at the Center of 20-mm Thick Sample No. 8 . . . . .	15
5.	Average Front and Back Surface Temperatures Above Ambient at the Center of 5-mm Thick Sample No. 3 . . . . .	16
6.	Average Front and Back Surface Temperatures Above Ambient at the Center of 5-mm Thick Sample No. 4 . . . . .	17
7.	Front View of Ballistic Clamp Fixture . . . . .	19

8.	Modified Remington 700 Rifle With 40-mm Smooth Bore Fragment Launcher Attachment . . . . .	20
9.	Modified Remington 700 Rifle Assembled and Secured in Firing Bracket Next to Doppler Radar Head . . . . .	20
10.	Average Front and Back Surface Temperatures Above Ambient at the Center of 5-mm Thick Fabric No. 1 . . . . .	26
11.	Average Front and Back Surface Temperatures Above Ambient at the Center of 5-mm Thick Fabric No. 2 . . . . .	26
12.	Average Front and Back Surface Temperatures Above Ambient at the Center of 15-mm Thick Fabric No. 5 . . . . .	27
13.	Average Front and Back Surface Temperatures Above Ambient at the Center of 20-mm Thick Fabric No. 5 . . . . .	27
14.	Average Front and Back Surface Temperatures Above Ambient at the Center of 20-mm Thick Fabric No. 7 . . . . .	28
15.	Average Front and Back Surface Temperatures Above Ambient at the Center of 25-mm Thick Fabric No. 9 . . . . .	28
16.	Back Surface Temperatures Above Ambient at the Center of 5-mm Thick Sample No. 1 Versus That of the Kevlar Fabric Backing Layers 1, 2, and 3 . . . . .	29
17.	Back Surface Temperatures Above Ambient at the Center of 5-mm Thick Sample No. 2 Versus That of the Kevlar Fabric Backing Layers 1, 2, and 3 . . . . .	29
18.	Back Surface Temperatures Above Ambient at the Center of Back Center of 5-mm Thick Sample No. 3 Versus That of the Kevlar Fabric Backing Layers 1, 2, and 3 . . . . .	30
19.	Back Surface Temperatures Above Ambient at the Center of Back Center of 5-mm Thick Sample No. 4 Versus That of the Kevlar Fabric Backing Layers 1, 2, and 3 . . . . .	30
20.	Back Surface Temperatures Above Ambient at the Center of 15-mm Thick Sample No. 5 Versus That of the Kevlar Fabric Backing Layers 1, 2, and 3 . . . . .	31
21.	Back Surface Temperatures Above Ambient at the Center of 20-mm Thick Sample No. 6 Versus That of the Kevlar Fabric Backing Layers 1, 2, and 3 . . . . .	31
22.	Back Surface Temperatures Above Ambient at the Center of 20-mm Thick Sample No. 7 Versus That of the Kevlar Fabric Backing Layers 1, 2, and 3 . . . . .	32
23.	Back Surface Temperatures Above Ambient at the Center of 20-mm Thick Sample No. 8 Versus That of the Kevlar Fabric Backing Layers 1, 2, and 3 . . . . .	32
24.	Back Surface Temperatures Above Ambient at the Center of 25-mm Thick Sample No. 9 Versus That of the Kevlar Fabric Backing Layers 1, 2, and 3 . . . . .	33
25.	Pusher Plate and 1-lb Steel Fragment With Polymer Foam Sabots Attached on Both Ends . . . . .	38

26.	Blanket Clamped in Frame Impacted by a 454-g Steel Fragment . . . . .	39
27.	Typical Damage on a Ply of Kevlar as a Result of Impact by a 454-g Steel Fragment . . . . .	39
28.	Typical Damage on an Inner Ply of Silica Oxide as a Result of Impact by a 454-g Steel Fragment . . . . .	40
29.	Fully Assembled Sub-scale Prototype MST Blanket . . . . .	40
30.	Live Propellant Experiment on an Uncovered Inert Acceptor Ammunition Crate . . . . .	41
31.	Side Burn Propellant Experiment (0.5 kg JA2) on a Covered Inert Acceptor Ammunition Crate . . . . .	41
32.	Temperature Profile of a Covered Acceptor Ammunition Crate . . . . .	42
33.	Temperature Profile of an Uncovered Acceptor Ammunition Crate . . . . .	43
34.	Typical Charred Remains of a Top-Burn Live Propellant Experiment . . . . .	43
35.	Setup of Bonfire Experiment Before Ignition . . . . .	44
36.	Bonfire Experiment Several Minutes After Ignition . . . . .	44
37.	Bonfire Experiment After the Flames Self-Extinguished . . . . .	45
38.	Temperature Profile of a Bonfire Experiment . . . . .	45
39.	Setup of Uni-charge Experiment, in Which Four Uni-charge Packages Were Placed Inside the Steel Tube . . . . .	46
40.	Setup of Uni-charge Experiment, Showing Stand-off Distance . . . . .	46
41.	Results From a Uni-charge Experiment . . . . .	47
42.	Back Surface of a Blanket Subjected to a Hot Gas Jet Emitted From Four Uni-charge Packages . . . . .	47
43.	Temperature Profile of the Back Surface of a Blanket From a Uni-charge Experiment . . . . .	48
44.	Uni-charge Placed on Top of a Covered Inert Acceptor Before Ignition . . . . .	49
45.	Uni-charge Placed on Top of a Covered Live (Uni-charge) Acceptor Before Ignition . . . . .	49
46.	Typical Results From the Ignition of a Uni-charge on Top of an MST Blanket . . . . .	49
47.	Temperature Profile Results From the Ignition of a Uni-charge on Top of an Undamaged MST Blanket (four plies of Kevlar ) . . . . .	50
48.	Temperature Profile Results From the Ignition of a Uni-charge on Top of an Undamaged MST Blanket (five plies of Kevlar ) . . . . .	50
49.	Temperature Profile of a Live Acceptor Under a Torn Blanket With a Uni-charge Ignited onTop (four layers of Kevlar ) . . . . .	51
50.	Temperature Profile of a Live Acceptor Under a Torn Blanket With a Uni-charge Ignited onTop (five layers of Kevlar ) . . . . .	51
51.	Instrumented Acceptor Stack of Ammunition After Several Experiments . . . . .	52



52.	The Effect of Stitching on the Brittle Ceramic Felt Material . . . . .	52
53.	Composite Sandwich Schematic Showing Different Layers of Material . . . . .	53

## Tables

1.	Thermal Properties of NASA's Thermal Protective System for Atmospheric Entry and Hypersonic Cruise Vehicles . . . . .	3
2.	Commercially Available Fabrics for Use in Sample MST Blankets . . .	5
3.	Organic Ballistic Fiber Material Properties . . . . .	6
4.	Sample MST Blankets Used in the Flame Penetration Experiments . .	9
5.	Sample MST Blankets for the Heat Penetration Experiment . . . . .	13
6.	Baseline Experiments With Short Exposure Duration of the Unpainted Sample Surface . . . . .	14
7.	Flame Penetration Into a Thick Wood Block With a Smaller Sample . .	23
8.	Flame Penetration Into a Thin Wood Block With a Smaller Sample for 10 Seconds' Exposure . . . . .	24
9.	Flame Penetration Into a Thin Wood Block With Larger Samples for 10 Seconds' Exposure . . . . .	25
10.	Maximum Temperature of the Front Surface of the Sample and Back Surface of the Third Kevlar Fabric Layer . . . . .	34
11.	Estimated Effective Thermal Diffusivity Values of Sample MST Blankets . . . . .	35
12.	Estimated Back Surface Temperatures of the Third Layer of Kevlar Fabric . . . . .	37
13.	Areal Density of Kevlar Ballistic Blankets . . . . .	37
14.	Typical Fragment Velocities, Calibration Data of Fragment Launcher, and Penetration Data . . . . .	38
15.	Weight and Cost Estimates for MST Blanket, BPS Blanket, and a BPS-Ceramic Hybrid Solution . . . . .	54

# FIRE-RESISTANT AND FRAGMENT PENETRATION-RESISTANT BLANKETS FOR THE PROTECTION OF STORED AMMUNITION

---

## 1. Introduction and Background

---

Munitions stored in the open are vulnerable to a host of threats, both friendly and hostile in nature. The U.S. Army Defense Ammunition Logistics Activity (AMMUNITIONLOG) tasked key players at the U.S. Army Research Laboratory (ARL) to design and evaluate a protection scheme comprised of a rapidly deployable system of barricades and fire-inhibiting blankets as a part of the Munitions Survivability Technology (MST) program. These barricades and blankets will prevent the propagation of reactions and fire between stacks of stored munitions.

When large quantities of ammunition are stored outdoors, the deflagration of one stack can lead to the detonation of adjacent stacks by various mechanisms such as direct fragment impact from high velocity low trajectory projectiles, blast pressure, rapid deformation, and burning because of fire propagation.

In order to prevent most of these mechanisms, the individual stacks of ammunition can be separated by either large distances or earthen barricades, which will prevent direct fragment impact. Although a barricade may separate stacks of ammunition, detonations may still occur by indirect means such as hot fragments, firebrands, and burning propellant from the donor stack. These become high trajectory low velocity projectiles and may land on neighboring acceptor stacks of ammunition. If the acceptor stack contains easily ignitable material such as propellant, ammunition crates constructed of wood, or combustible cartridge cases, a fire and subsequent low order detonations are possible. A domino effect can destroy large stores of munitions in the course of hours or even days. In order to protect against these indirect mechanisms, a fire-blocking and heat-blocking blanket with a specific level of ballistic protection can be used to cover the ammunition stack.

There is an extensive historical database to justify this research effort, some of which is mentioned in ARL-TR-2030 [1]. Frey and Starkenberg cite instances when sequential detonations led to the loss of entire storage depots of ammunition. These depots were lost because of alleged sympathetic detonation from neighboring ammunition stacks that tend to expel firebrands, unexploded/armed warheads, and assorted hot fragments. These fire initiators can be thrown great distances, even farther than the mandated minimum safe distances for ammunition storage. Because of this, there is the potential for long burn periods for an ammunition depot fire when firebrands are randomly

thrown toward neighboring stacks. The earthen barricades and blankets evaluated in the MST program should greatly increase the overall survivability of an ammunition depot if they are used in concert and properly implemented.

This document only illustrates the work performed in the development of the fire- and heat-blocking/ballistic blanket portion of the program. Past studies that looked at the usefulness of fire-blocking materials demonstrated mixed results for the effectiveness of blankets in preventing fire propagation [2]. This study, however, was not specifically focused on a blanket solution, and a full spectrum of experiments was not performed to adequately assess a blanket's effectiveness in preventing fires and sympathetic detonations.

Through laboratory scale flammability study and sub-scale field experiments, ARL hoped to develop a lightweight MST blanket to protect stored munitions from low velocity, high trajectory ballistic threats as well as an assortment of fire threats when the blanket is used in conjunction with a barricade system.

In order to develop this blanket, a number of design issues had to be taken into consideration. The blanket should protect against a wide range of low velocity ballistic as well as multiple thermal threats. These threats were determined, based on best guess estimates from empirical data as well as real-world events, but because of the statistical nature of an exploding munitions stack, all the potential combinations of threats could not be evaluated. The system had to be flexible enough to conform to any size pallet of munitions, so a modular approach to the design was chosen. The individual pieces from this modular design had to be easily handled and assembled by soldiers in the field. The system also had to be durable and manufactured from high performance, low cost materials. Based on these requirements, a large number of candidate materials had to be evaluated to develop the most robust and cost-effective solution.

A literature search was performed for the pertinent information about the resistance to flame and heat penetration of single and multiple layers of various organic and inorganic fiber-based fabrics. A total of about 150 relevant papers and reports were found. Many studies indicated that resistance to flame and heat penetration increased when layers of fabrics made from fibers of organic and inorganic polymers were used [3-14].

An example of the use of a combination of inorganic fiber-based fabrics is the heat-blocking system used by the National Aeronautics and Space Administration (NASA) for the thermal protection of atmospheric entry and hypersonic cruise vehicles [7]. The front and the back surfaces of the heat-blocking system consist of four layers of alumino-borosilicate (ABS) fabric with a fifth inner layer of silica fabric and thread. The core consists of a combination of layers of the following materials: (a) silica felt (98.5% SiO<sub>2</sub>), (b) ABS (62% Al<sub>2</sub>O<sub>3</sub>,

14% B<sub>2</sub>O<sub>3</sub>, and 24% SiO<sub>2</sub>), (c) silica felted fiber mat (99.9% SiO<sub>2</sub>), (d) alumina mat (95% Al<sub>2</sub>O<sub>3</sub>, 5% SiO<sub>2</sub>, and (e) silica felt (98.5% SiO<sub>2</sub>). The thermal properties of the five layers that constitute the core are listed in Table 1.

Table 1. Thermal Properties of NASA's Thermal Protection System for Atmospheric Entry and Hypersonic Cruise Vehicles<sup>a</sup>

Layers	Material	Density (kg/m <sup>3</sup> )	Heat Capacity (kJ/kg-K)	Thermal Conductivity (kW/m-K) x 10 <sup>5</sup>	Thermal Diffusivity (mm <sup>2</sup> /s) <sup>b</sup>
1	Silica felt (98.5% SiO <sub>2</sub> )	96	0.349	1.58	0.47
2	ABS (62% Al <sub>2</sub> O <sub>3</sub> , 24% SiO <sub>2</sub> , 14% B <sub>2</sub> O <sub>3</sub> )	96	0.388	2.16	0.58
3	Silica felted fiber mat (99.9% SiO <sub>2</sub> )	136	0.258	1.87	0.53
4	Alumina mat (95% Al <sub>2</sub> O <sub>3</sub> , 5% SiO <sub>2</sub> )	96	0.336	1.80	0.56
5	Silica felt (98%SiO <sub>2</sub> )	96	0.349	1.58	0.47

<sup>a</sup>taken from [5]; b: thermal diffusivity = thermal conductivity/(density)(heat capacity)

The data in Table 1 indicate that thermal diffusivity values for inorganic fiber-based fabrics are between 0.47 to 0.58 mm<sup>2</sup>/s. The inverse of thermal diffusivity can be considered as a parameter expressing resistance to heat penetration. The combination of alumina- and silica-based fabrics would be a likely candidate for sample MST blankets, since the combination has low thermal diffusivity values.

An example of the use of combination of organic and inorganic polymer fiber-based fabrics is the system used for the Columbia space shuttle [9]. The system consisted of silicone-impregnated fiberglass batting, sewn in covers of reinforced polyimide film, with alternate layers of perforated polyimide film and Dacron (polyethylene terephthalate [PET]) net, and a polyimide film cover. This combination had also been considered for high temperature filtration, flame-resistant upholstery for commercial passenger vehicles, and aircraft crew uniforms.

Combinations of organic and inorganic fibers are also used to enhance resistance to fuselage "burn-through" in aircraft fuel fires [15]. Fuselage burn-through refers to the penetration of an external post-crash fuel fire into an aircraft cabin.

The time to burn through is critical because, in survivable aircraft accidents, the hazards of burning cabin materials ignited by burn-through from an external fuel fire may incapacitate passengers before they are able to escape.

There are typically three barriers that a fuel fire must penetrate in order to burn through to the cabin interior: the aluminum skin (30 to 60 seconds' resistance, depending on thickness), the thermal acoustical insulation, and the interior side wall and floor panel combination. Thermal acoustical insulation, typically comprised of fiberglass batting encased in a polyvinylfluoride ([PVF], Tedlar ) moisture barrier, provides 60 to 120 seconds' protection as long as it is not dislodged from the fuselage structure. Honeycomb sandwich panels used in the side wall and floor areas of transport aircraft offer a substantial barrier to fire.

The efficiency of preventing or delaying burn-through of modified fiberglass batting or replacement insulation materials has been examined in full-scale fire experiments with a reusable fuselage rig [15]. The use of polyimide (Kapton ) film (an organic polymer) in place of PVF (Tedlar ) film improved the burn-through resistance. A layer of Nextel (tightly woven ABS fabric) is placed inside each of the insulation batts, and all are encapsulated in the standard metallized PVF (Tedlar ) film; this prevented burn-through for nearly 7 minutes. Most of the Nextel remained in place except for one area about 20 inches by 20 inches (0.51 m by 0.51 m), which had been penetrated.

Additional organic and inorganic polymer fibers as insulation materials evaluated in full-scale fire experiments with a reusable fuselage rig consisted of [15]

- Curlon - a heat-treated, oxidized polyacrylonitrile fiber (OPF) (70% carbon, 20% nitrogen, and 10% oxygen). Curlon was extremely effective in resisting flame penetration for at least 5 minutes during several full-scale experiments.
- Solimide AC-430 System - the system consisted of rigid polyimide foam, with Quartzel , a vitreous silica wool barrier. This system, however, was less effective than the system with Nextel™-enhanced fiberglass and the Curlon .
- AstroquartzII System - the system consisted of an AstroquartzII ceramic mat with a thin layer of Nextel™ ceramic fiber paper. This system resisted flame penetration for more than 8 minutes.

The Federal Railroad Administration [9] has also successfully tested glass fiber, ceramic fiber, and mineral fiber blankets for the thermal protection of aluminum railroad tank cars from torch and pool fires.

The use of organic and inorganic fiber-based fabrics has now been commercialized for variety of applications [10-14]. Table 2 lists some commercially available fabrics that could be considered for the sample MST blankets. The amount of organic polymer fibers is very small compared to inorganic polymer fibers. For example, Nextel™ 312 sewing threads are a combination of Nextel™ 312 ceramic fibers and rayon fibers (10% by weight) [13]. The list is not a comprehensive list; it is only an example of commercially available fabrics for use as sample MST blankets for thermal protection. Please note that these fabrics do not provide protection from ammunition penetration.

Table 2. Commercially Available Fabrics for Use in Sample MST Blankets

Fabrics and Exposure Temperature Limit <sup>a</sup>	Ref
1) Zetex , T 593° C (inorganic fibers); 2) Zetex Plus , T 1093° C (inorganic fibers)	10
1) Kao-Tex™ 2000 cloth, T 1093° C (inorganic fibers); 2) calcium magnesium silicate, T 958° C; 3) Kaowool ceramic fiber, B Blanket, T 958° C (inorganic fibers); 4) Cerawool , T 958° C (inorganic fibers); 5) Kaowool blanket S, T 1230° C (inorganic fibers); 6) Cerachem blanket, T 1430° C (inorganic fibers)	11
1) Duraback™, T 958° C (inorganic fibers); 2) Durablanket 2600, T 1430° C (inorganic fibers)	12
1) Nextel™ 312 ceramic fibers, T 1430° C (aluminoborosilicate); 2) Nextel™ 440 ceramic fibers, T 1648° C (aluminoborosilicate)	13
RM Therma-Shield insulation materials: 1) SuperSpan welding cloth; 2) Fluorel™-coated ceramic cloth 1093° C; 3) Therma-Shield 2400 (alumina silica fiber with binders) 1288° C	14

<sup>a</sup>Detailed chemical compositions of the fabrics are not available, as they are proprietary materials. Temperature specifications are from the manufacturer's brochures.

There were several options from which to choose in off-the-shelf technology for high performance fibers, which may be used in a flexible blanket for ballistic applications. These fibers include para-aramid fibers and ultrahigh molecular weight polyethylene (PE) fibers. DuPont (Kevlar®) and Acordis (Twaron ) both produce para-aramid fibers, while Honeywell (Spectra ) and Toyobo (Dyneema ) produce PE fibers. Both families of fibers offer unparalleled strength and stiffness-to-weight ratios (see Table 3) and are widely used in ballistic applications [17-18].

Table 3. Organic Ballistic Fiber Material Properties

Material	Upper Use Temp (°C)	Density (g/cc)	Tenacity (g/den)	Tensile Strength (MPa)	Elongation (percent)	Cost (\$/lb)
Aramid	300	1.44	23 to 26	2760	2.4 to 3.6	30
Polyethylene	120	0.97	28 to 38	3000	3.0 to 4.5	30
Nylon	150	1.14	9	76	10	5 to 10

These fibers need to be woven into the proper architecture in order to see their full benefits. Mackiewicz [19] examined the performance of several different weave architectures and determined that the Kevlar® 29 Style #745 [20] weave provided optimal protection from overhead artillery blasts and associated fragments. Based on this research, the U.S. Army developed a ballistic protective system (BPS) to protect materiel [21] from ballistic threats. This BPS blanket was chosen as a starting point for the MST blanket, but since it offered too much ballistic protection and too little flame protection, modifications had to be implemented.

## 2. Experimental

### 2.1 Fibers/Fabrics

Because of the diverse performance requirements of the blanket, several organic and inorganic fibers/fabrics had to be examined in a composite sandwich construction whereby the optimal properties of each material could be exploited. Some of the materials evaluated had to meet certain ballistic requirements; these include several fabrics woven from high performance organic fibers such as ballistic nylon, para-aramid, and polyethylene fibers. Other materials needed to meet the high temperature requirements of the blanket; they consisted of several candidate fabrics woven from inorganic fibers, including fiberglass and ceramic fibers. Several other materials and/or coatings had specific performance requirements such as flame resistance, abrasion resistance, water resistance, and camouflage properties.

### 2.2 MST Blanket Specimens

The specimens evaluated in this study fell into three categories in size and construction. Small (< 305 mm by 305 mm) coupons were constructed of several layers of fabric stacked to achieve a desired thickness. These samples were typically used in small-scale laboratory flammability studies, where they were

clamped in some type of fixture and exposed to a thermal threat. Large (>610 mm by 610 mm) specimens were also fabricated for ballistic study. These composite blankets of varying thickness consisted of multiple layers of organic and inorganic fabrics, which were mounted in a frame for fragment penetration experiments. The third type of specimen fabricated consists of a sub-scale finished product, which was designed to cover a generic ammunition crate that is 915 mm wide by 915 mm long by 305 mm high. These sub-scale demonstrators were constructed of five pieces (one top and four sides) that are held securely together with a series of straps and buckles to completely cover the ammunition crate.

## **2.3 Flammability**

The objective of the study was to examine the resistance to flame and heat penetration by a combination of inorganic and organic fiber fabrics. A literature search indicated that inorganic fiber-based fabrics have high fire resistance and a combination of organic and inorganic fiber-based fabrics in layers is effective for thermal and weather protection. Contact was made with several high performance blanket manufacturers who are using technology developed by NASA. Consequently, some of these manufacturers supplied ARL with some of these high performance fabrics that have a thickness of 5 mm (defined as thin in this report) and 15 to 25 mm (defined as thick in this report). These high performance fabrics are identified as sample MST blankets in this report. The resistance of each sample MST blanket to flame and heat penetration was assessed in the following types of experiments:

### **2.3.1 Flame Penetration Experiments**

An oxyacetylene torch flame was used in the experiments. The top surface of the sample MST blanket wrapped around a wooden block was exposed to the oxyacetylene flame. The extent of burn-through of the sample blanket and wood and the charring and flaming of wood were used to assess the extent of flame penetration through the sample MST blanket.

### **2.3.2 Heat Penetration Experiments**

The front surface of the sample MST blanket on top of three layers of Kevlar fabric (as a backing fabric) was exposed to a known external heat flux value. Temperatures measured at the center of the front and back surfaces of the sample MST blanket and back surfaces of each layer of the Kevlar fabric were used to assess the extent of heat penetration through the sample blanket.

## **2.4 Flame Penetration Experiments**

In the flame penetration experiments, a sample surface mounted on a block of wood was exposed to an Airco oxyacetylene torch with a No. 144-2 cutting tip. In some experiments, a black powder propellant or M9 propellant was placed between the sample and wood surface. The oxygen and acetylene gas pressures



on the torch were set at 276 kPa and 34 kPa, respectively. The tip of the flame was kept between 13 and 25 mm above the center of the sample surface. Some samples ignited as soon as the oxyacetylene flame was brought close to the surface. In these experiments, samples were allowed to burn for about 10 seconds. Flame penetration depths and visual observations were made during the study of the samples. Three sets of experiments were performed in which samples dimensions, the thickness of the wooden block, and the mode of attachment were varied:

#### **2.4.1 First Set of Experiments (thick wooden block, metal frame)**

In this set of experiments, 152-mm square samples were used. The samples were mounted on top of a 152-mm square and 51-mm thick block of pine. A 6-mm thick metal picture frame fixture with a 102-mm square opening was placed on top of the sample surface to keep it stable during the experiment. The sample was studied until failure for 3 to 80 seconds.

#### **2.4.2 Second Set of Experiments (thin wooden block, metal frame)**

In this set of experiments, 152-mm square samples were used. The samples were mounted on top of a 190-mm square and 19-mm thick blocks of pine. A 6-mm thick metal picture frame fixture with a 102-mm square opening was placed on top of the sample surface to keep it stable during the experiment. The sample surface was exposed to the flame for 6 to 10 seconds.

#### **2.4.3 Third Set of Experiments (larger sample area, thin wooden block, and no metal frame)**

In this set of experiments, 254-mm square and 152- by 356-mm rectangular samples were used. The samples were stapled on top of 190-mm square and 19-mm thick and 140- by 152-mm and 38-mm thick blocks of pine, respectively. The sample surface was exposed to the flame for 6 to 10 seconds. The sample MST blankets used in the flame penetration experiments are listed in Table 4.

### **2.5 Heat Penetration Experiments**

For the heat penetration experiments, the sample MST blankets, which consisted of combinations of mostly alumina, silica, and ceramic-based fabrics (inorganic fabrics) with a backing made of three layers of Kevlar fabric (organic fabric), were used. The selection of sample MST blankets was based on the data from the flame penetration experiments and background information from the literature. Spectra PE material was excluded from these experiments because of inherently poor flammability properties. The sample MST blanket was evaluated in a heat penetration apparatus shown in Figure 1.

Table 4. Sample MST Blankets Used in the Flame Penetration Experiments

Sample	Name <sup>a</sup>	Description <sup>a</sup>
A	Silica cloth 399C-1	94% silica; service temperature: as hot as 2000° F (continuous heating) and 3000° F (short term heating); weight: 18 oz/yd <sup>2</sup> ; thickness: 0.030 in. Cotronics Corp., Brooklyn, NY
B	Felt insulation 370-1	Silica fibers; service temperature: as hot as 2300° to 3000° F; density: 12 lb/ft <sup>3</sup> for a thickness of 0.13 in. and 8 lb/ft <sup>3</sup> for a thickness of 0.25 in. Cotronics Corp., Brooklyn, NY
C	HTX-1000-9N	94% silica similar to A but thicker - a woven continuous filament amorphous silica fabric with a proprietary coating; service temperature: as hot as 1800° F; weight: 33 oz/yd <sup>2</sup> ; thickness: 0.046 in. Amatex Corporation, Morristown, PA.
D	Nextel 312 (AF 40)	Woven from continuous alumino-borosilicate fibers; service temperature: as hot as 2200° F (continuous) and 2600° F (short term); weight: 25.0 oz./yd <sup>2</sup> ; thickness: 0.039 in.; melting point: 3272° F. 3M Company, St. Paul, MN.
E	Siltemp 25M Mat	96% silica high temperature insulation made from amorphous silica; service temperature: as hot as 2000° F; density: 13 lb/ft <sup>3</sup> ; nominal thickness of 0.23 in. Ametek, Wilmington, DE
F	Kevlar®/fiber glass 22PT30	Medium weight aramid fiber blends over a fiberglass yarn; service temperature: as hot as 650° F; weight 22 oz/yd <sup>2</sup> ; thickness: 0.060 in. Amatex Corporation, Morristown, PA.
G	Nomex® III aramid blend	Weight: 7.5 oz/yd <sup>2</sup> . Southern Mills, Union City, GA
H	Fiberglass	Woven ceramic fibers; weight: 24 oz/yd <sup>2</sup> ; thickness: 0.025 in. JPS Glass Company, Slater, SC
I	Silicone-coated silica cloth HT 1000-9N-SRI	94% silica woven continuous filament amorphous silica fabric with silicone rubber coating on one side; service temperature: as hot as 1800° F; weight: 42 oz/yd <sup>2</sup> ; thickness: 0.054 in.; Amatex Corporation, Morristown, PA.
J	NorFab Kevlar	- glass style 30PT20DC, 30 oz/yd <sup>2</sup>
K	3M Nextel	fabric style 440
L	Ceramic fabric	style 399C-2
M	Ceramic fiber batting	370-1; 1/8 in.
N	Ceramic fiber batting	370-4; 0.5 in.
O	Ballistic blanket	- 13 layers of Kevlar fabric
P	Kevlar -Nomex	fabric style 5450; 9.2 oz/yd <sup>2</sup>
Q	Amatex mineral-coated glass	style G26T33-7B; 9.2 oz/yd <sup>2</sup>
R	Carbon fiber batting	; 7 oz/yd <sup>2</sup>

<sup>a</sup>Names and information are from the manufacturers' brochures; the units are the same as reported in the brochures.

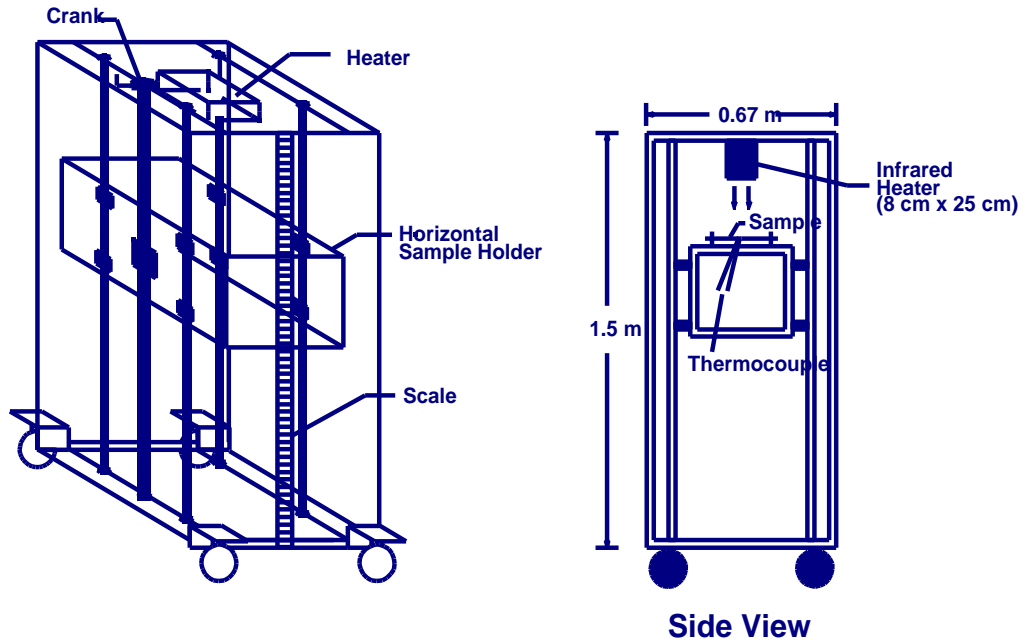


Figure 1. Heat Penetration Apparatus Used in the Experiments for Sample MST Blankets.

The heat penetration apparatus consisted of a single infrared heater (Model 5208-10, Research Inc., Minneapolis, MN) attached at the top of a 1.5-m high, 0.67-m long, and 0.67-m wide metal frame with wheels. The heater had a cross section of 80 mm by 250 mm. A controller (Model 5620, Research Inc., Minneapolis, MN) was used to adjust the output of the radiant heater.

A horizontal platform was used to hold the sample MST blanket. The platform was moved in a vertical direction to change the external heat flux value at the sample surface. A Medtherm heat flux gauge was used to calibrate the heat flux from the radiant heater to the sample surface. The calibration is shown in Figure 2. The heat flux increases with decreasing distance between the sample surface and the radiant heater and reaches a maximum of about  $200 \text{ kW/m}^2$  for a distance of 30 mm between the sample surface and the heater.

In each experiment, the sample MST blanket with three layers of Kevlar fabric at the back was placed on top of the horizontal platform, as shown in Figure 3. Five thermocouples at the center of each layer were used to measure (a) the front and back surface temperatures ( $T_s$  and  $T_u$ , respectively) of the sample MST blanket, and (b) the back surface temperatures of each layer of the Kevlar fabric ( $T_{k1}$ ,  $T_{k2}$ , and  $T_{k3}$ ). A water-cooled shield was used to block the heat exposure of the sample blanket until the radiant emission from the heater was stabilized (20 seconds).

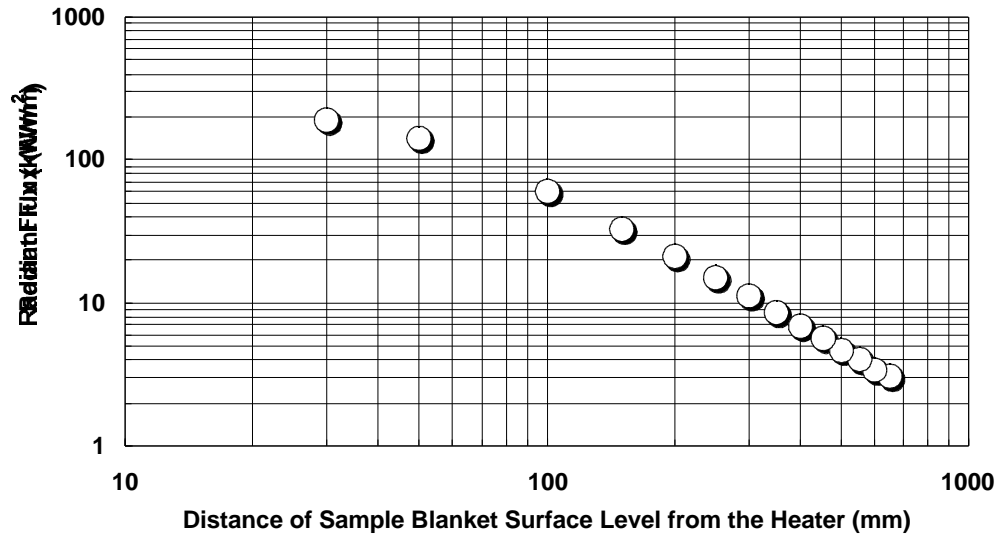


Figure 2. Measured Radiant Heat Flux at the Sample Surface Versus Distance Between the Surface and the Radiant Heater in the Heat Penetration Apparatus.

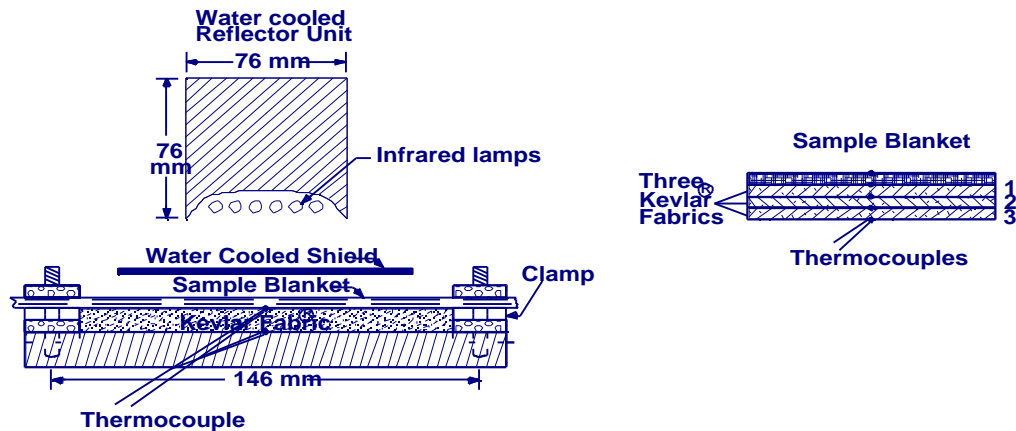


Figure 3. Arrangement of the Sample MST Blanket With Three Layers of Kevlar Fabric at the Back of the Sample MST Blanket on the Horizontal Platform of the Heat Penetration Apparatus.

For the temperature measurements, K-type thermocouples (Omega) were used, which were attached to the fabric surfaces with a high temperature adhesive. The thermocouples were connected to a data processor (Analog Device, Signal Processor Model 5B47-K-04). The data processor was connected to a data logger (DL1, prototype unit) interfacing with a Gateway 2000 PC with Windows 95

operating system through its serial communication port. A software package LITEUP was used to instruct the hardware to read the data. The software package LITESHOW was used to stop the data acquisition and transfer the data into a data file. The software package XLITE was used to convert the data file to a text file. The K-type thermocouple data were imported as voltages and converted to degrees C (conversion factor of degrees C per 40 microvolts).

The experiment was started by placing the sample MST blanket on the horizontal platform, turning on the data processor, data logger, and the Gateway 2000 PC, and initiating the software package LITEUP with the name of the data file. The heater was then turned on with the water-cooled shield in place to block the heat exposure of the sample MST blanket. The heater was allowed to stabilize for 20 seconds, at which time, the water-cooled shield was moved away and the sample MST blanket surface was exposed to the preset heat flux value. In each experiment, the sample blanket was exposed to heat flux for a fixed exposure time (between 10 to 120 seconds). The temperature was measured every 0.05 second at five locations (at the center of the front and back surfaces of the sample MST blanket and back surfaces of the three layers of Kevlar fabric).

At the end of the exposure, the heater was turned off. The software application LITESHOW canceled the data acquisition and transferred the data into a data file. The PC was then booted in DOS (disk operating system), and the software XLITE converted the data file into a text file. The PC was then reverted to Windows 95 and the text file was read into a Microsoft Excel template worksheet. The thermocouple data imported as voltages were converted to degrees C and recorded into the Microsoft Excel temperature worksheet as a 1-second running average (temperature was recorded every 0.05 second and thus averaged 20 data points).

The sample MST blankets evaluated in the heat penetration apparatus are listed in Table 5. Note that the samples consist of layers of alumina, silica, and other inorganic materials. These fabrics were similar to those listed in Tables 1 and 2. Combinations of numbers 1000, 800, and 600 designate various types of fiberglass. CH represents silica fiber. Nextel consists of woven aluminoborosilicate (ABS) fibers.

Four sample MST blankets were thin (5 mm) and five sample MST blankets were thick (15 to 25 mm). The manufacturers did not provide detailed chemical compositions of the samples because they were assembled from proprietary combinations of fabrics.

## **2.6 Determination of Exposure Conditions**

The goal of the sample MST blanket exposure experiments was to expose the surface to a high enough temperature for longer times, without ignition, and to

be able to use the data for extrapolation to higher temperatures (possibly as high as 3000° C) and exposures as long as 60 seconds.

Table 5. Sample MST Blankets for the Heat Penetration Experiment

Sample No.	Fabric Arrangement	Fabric Layers <sup>a</sup>	Thickness/ Side Exposed
<b>Thin sample MST blankets</b>			
1	Shiny	1000/600 aluminum; AF – 62 Nextel 1000/600 aluminum	5 mm thick
2	Beige	188 CH; 0.13-in. Kaowool paper rubberized silica	5 mm thick beige
3	Light green	Zetex 10615-1860; 0.13-in. Kaowool paper; 84 GHS	5 mm thick Zetex
4	Creamy	Ceramic fabric 399C-2 0.13-in. ceramic blanket	5 mm thick
	Creamy	Ceramic fabric 399C-2	
<b>Thick sample MST blankets</b>			
5	Shiny	1000/600 aluminum- Copper knit 500; 188 CH	15 mm thick beige
6	Silver silica	1000/500 stainless steel foil 0.5-in. Kaomat ; 188 CH	20 mm thick beige
7	Orange silicone	1000/500 OS <sup>b</sup> ; 0.5-in. 607 Superwool ; 188 CH	20 mm thick beige
8	Shiny	1000/800 aluminum; 0.5-in. Kaowool-S ;188 CH	20 mm thick beige
9	Fiberglass weave	1000/800 stainless steel foil; 0.5-in. 607 Superwool ; 1000/600 aluminum	25 mm thick fiberglass

<sup>a</sup>Sample details are from the manufacturer's catalogue.

<sup>b</sup>OS = orange silicone

Several preliminary experiments were performed to set the exposure conditions without the ignition of the sample. For the initial experiments, two thin sample MST blankets (No. 1, 3, and 4) and a thick sample MST blanket (No. 8) were used. The experiments were performed with unpainted surface and with a flat black painted surface. The sample surface was exposed to 20, 50, and 84 kW/m<sup>2</sup> for short (10 to 20 seconds), intermediate (100 seconds), and longer (120 seconds) exposure, when there was no ignition of the sample.

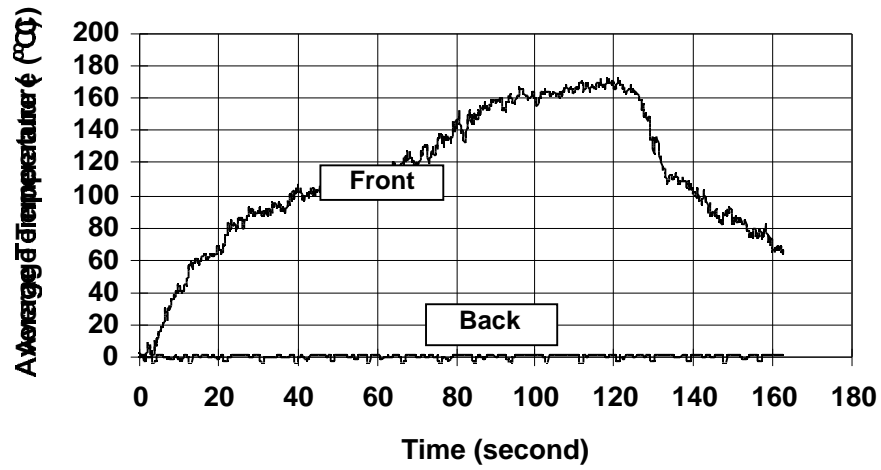
The first set of baseline conditions is listed in Table 6. The experiments were started with the short exposure to avoid the possibility of igniting the sample blanket. The sample blanket's surface was not coated. The short exposure of 10 to 20 seconds was found unsatisfactory as the temperature rise at the front surface of the sample MST blanket was quite low and the back surface temperature was close to ambient. Exposure for 100 seconds was also unsatisfactory.

Table 6. Baseline Experiments With Short Exposure  
Duration of the Unpainted Sample Surface

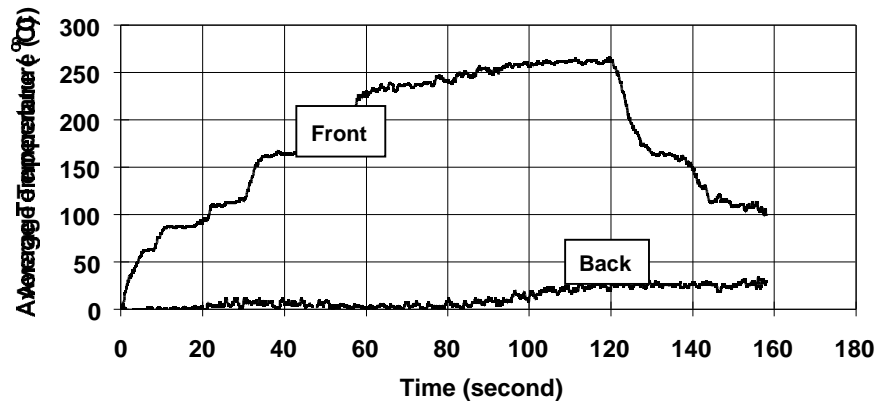
Experiment Number	Sample MST Blanket	Heat Flux (kW/m <sup>2</sup> )
1	1	20
2	1	20
3	1	50
4	4	20
5	4	50
6	4	50
7	4	84

The second set of baseline experiments used unpainted and black painted sample surfaces exposed to 84 kW/m<sup>2</sup> for 120 seconds. In the second set of experiments, samples 3, 4, and 8 were used. There was no sample ignition in any of the experiments. The data are shown in Figures 4 through 6.

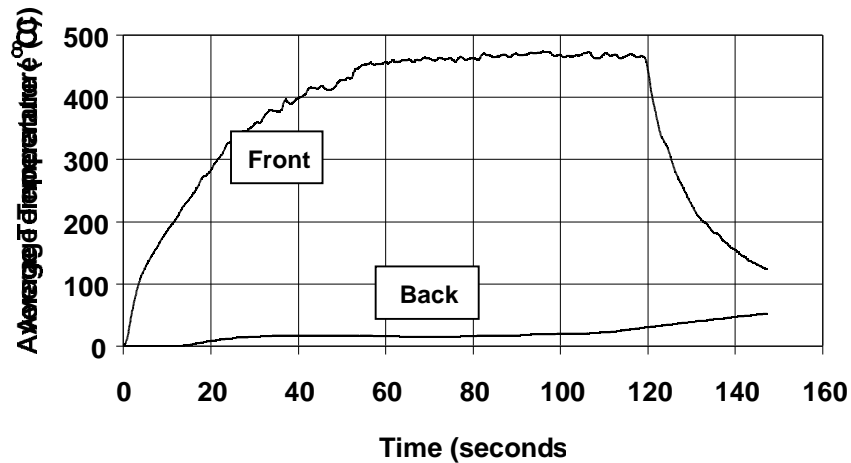
The surface temperature for the black painted surface is higher; the steady state is of longer duration, without the ignition of the sample. Data for the unpainted surface are unsatisfactory because of the low surface absorptivity. For example, an examination of the temperature profile for sample No. 8 in Figure 4 indicates that the surface temperature of the beige side (188 CH) is about 1.5 times the temperature of the shiny side (1000/800 aluminum, Figure 4a). Thus, an exposure of 84 kW/m<sup>2</sup> for 120 seconds of a flat, black painted surface was selected for the heat penetration investigation.



- a. Unpainted shiny side (1000/800 aluminum) was exposed to 84 kW/m² for 120 seconds.



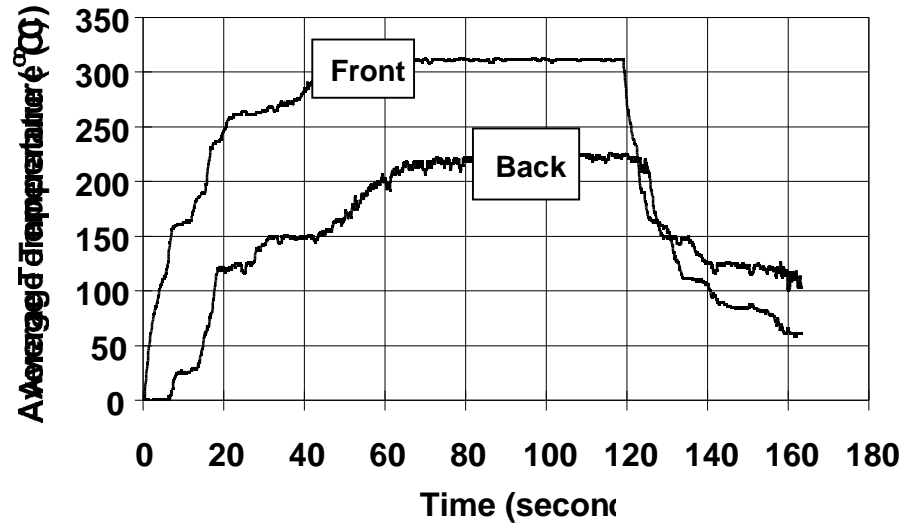
- b. Unpainted beige side (188 CH) was exposed to 84 kW/m² for 120 seconds.



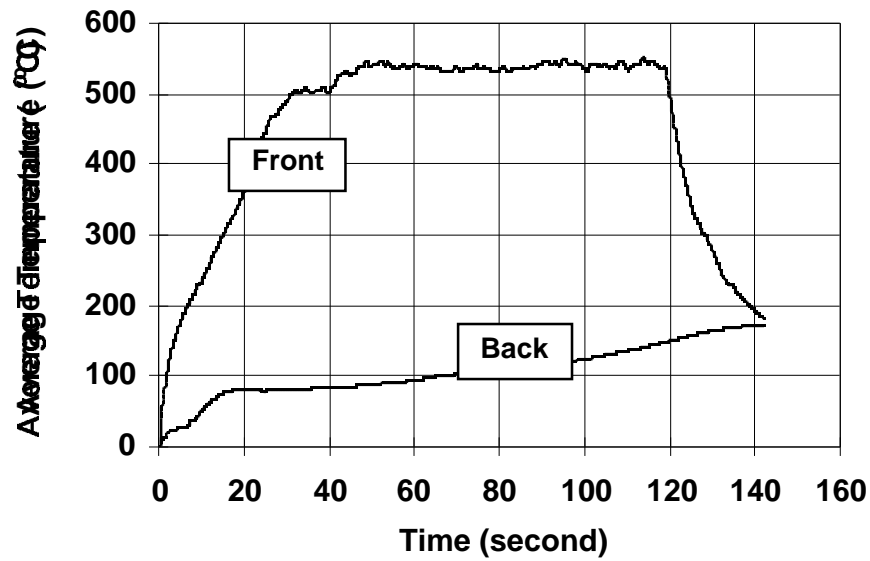
- c. Black painted beige side (188 CH) was exposed to 84 kW/m² for 120 seconds.

Figure 4. Average Front and Back Surface Temperatures Above Ambient at the Center of 20-mm Thick Sample No. 8.



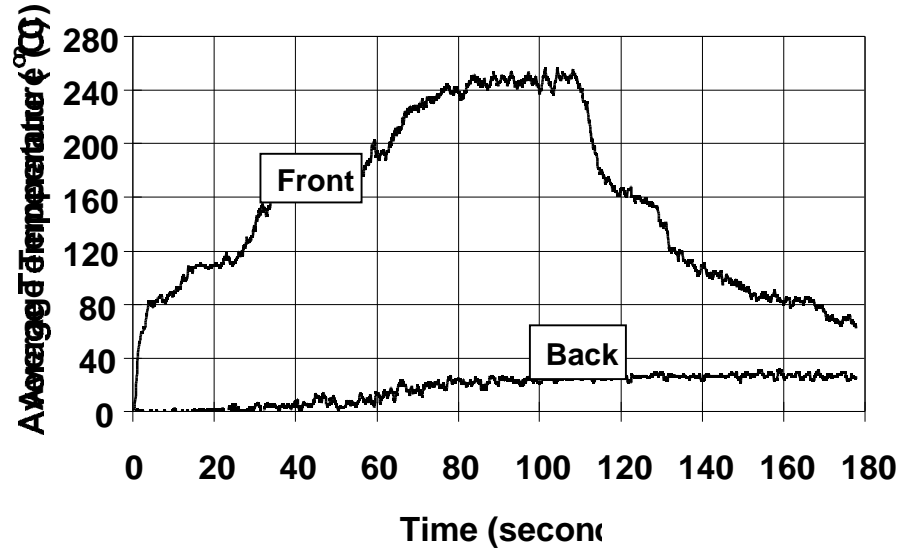


a. Unpainted surface was exposed to  $84 \text{ kW/m}^2$  for 120 seconds.

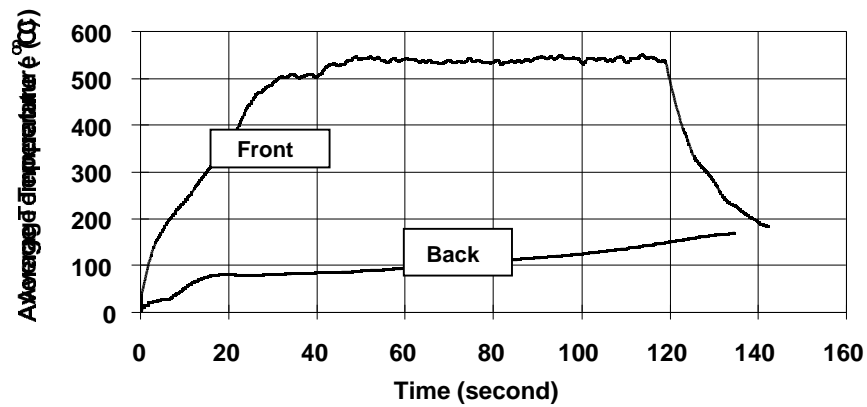


b. Black painted surface was exposed to  $84 \text{ kW/m}^2$  for 120 seconds.

Figure 5. Average Front and Back Surface Temperatures Above Ambient at the Center of 5-mm Thick Sample No. 3.



a. Unpainted surface was exposed to  $84 \text{ kW/m}^2$  for 120 seconds.



b. Black painted surface was exposed to  $84 \text{ kW/m}^2$  for 120 seconds.

Figure 6. Average Front and Back Surface Temperatures Above Ambient at the Center of 5-mm Thick Sample No. 4.

## 2.7 Resistance to Fragment Penetration

Two series of ballistic experimentation were performed in order to determine the ballistic performance of the hybrid blankets. The complete results of Phase 1 ballistic experimentation are documented in ARL-TR-2122 [22]. The results from the Phase 2 ballistics are presented in this report. This report also documents small-scale arena experiments in which these blankets were assessed against live propellant threats.

### 2.7.1 Phase 1 Ballistics

For this phase of ballistic experimentation, a 0.3-kg right circular cylinder was used as a fragment simulator. This simulator was 170 mm long and 17 mm in diameter. The fragment size was based on a series of experiments in which two Composition B (Comp-B) loaded M107 155-mm rounds were simultaneously nose detonated [22]. The resulting fragments were on the order of 0.3 kg and had an aspect ratio of 10. A right circular cylinder fragment simulator was chosen for ease of manufacturing and ease of launching.

The projectile fragments were launched from a 25-mm inner diameter smooth bore compressed gas gun. A polyethylene foam sleeve acted as a sabot to center the projectile in the gun barrel during firing. A polypropylene pusher plate made was used to provide a tight seal along the edges for efficient/repeatable projectile launching. The projectile velocity, which was based on the terminal velocity of a 0.3-kg falling body, was approximately 146 m/s. The velocity of the projectile was measured with break screens and high speed timers.

All the targets used for the Phase 1 ballistic study were fabricated from multiple layers of Kevlar 29 fibers. The inorganic fabrics were not expected to contribute to the ballistic performance of the system; therefore, they were not used in this phase of evaluation since the objective was to determine the blankets' ballistic effectiveness. Two different panel constructions were investigated, each with a different areal density, and are designated as ARL and FFF (Federal-Fabrics Fibers). All samples were stitched together with aramid thread and supported securely in a picture frame fixture according to MIL-C-44050A for fragment penetration experiments.

The 13.6-oz/yd<sup>2</sup> 17 by 17 (yarns/inch by yarns/inch) plain weave fabric used in the ARL targets was purchased from Hexcel-Schwebel (Anderson, South Carolina). The Style No. 745 fabric was woven from 3000-denier (weight in grams of a 9000-m-long end) Kevlar 29 yarn. The fabric was also treated with a waterproofing compound.

The Kevlar 29 yarns (fiber bundles) used in the fabrication of the FFF blankets were first bathed in a mixture of organic binder and vermiculite for flame resistance. After drying, the yarns were woven into a fabric for blanket construction and evaluation. This fabric was produced from 1500-denier yarns; therefore, the number of plies needed to achieve an equivalent areal density was more than enough. This weaving process resulted in a loose plain weave fabric, which was not as tightly woven as the ARL fabric. The areal weight of these fabrics with the vermiculite coating is approximately 4 oz/yd<sup>2</sup>, about one-third that of the ARL fabrics. Therefore, additional layers of FFF material were added to compare the blankets, based on equivalent areal densities.

All targets were secured between two 25-mm thick aluminum frames with C-clamps (see Figure 7). The samples were evaluated for ballistic performance with three shots per target in a diagonal array as illustrated. A 0.05-mm 2024-T3 aluminum sheet was used as a witness plate, and a “catch box” was positioned behind the target in order to stop any projectiles that completely penetrated the target..

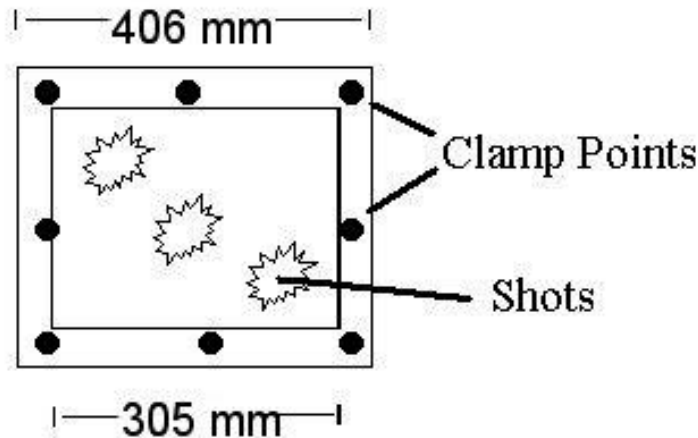


Figure 7. Front View of Ballistic Clamp Fixture.

### 2.7.2 Phase 2: Ballistics and Sub-Scale Arena Experiments

Based on the Phase 1 ballistics and the preliminary thermal evaluation, a plan for the Phase 2 ballistics and sub-scale arena experiments was developed. This would demonstrate the ability of aramid fiber/ceramic fiber blankets to provide flame protection and low velocity impact protection to co-located munitions from firebrands discharged by violent reaction of nearby ammunition stores. Phase 2 ballistics and sub-scale arena experiments were subdivided into three areas of effort to reach the objective. These controlled experiments were chosen because of the statistical nature of these events. If these blankets were set up in a full-scale arena experiment, any type of fragment impact or interaction with a thermal threat could not be guaranteed. In a controlled experiment, we could guarantee interaction and record all the appropriate data.

The first subdivision involved the Phase 2 ballistic investigation, in which different areal density Kevlar /silica oxide fabric targets were evaluated in order to determine an effective ballistic limit. This was performed with a larger fragment simulator traveling at a lower velocity than used in Phase 1 ballistics. The second and third subdivisions comprise the sub-scale arena experiments. The second subdivision involved static flame experiments with live propellant threats found in the field to determine a specific level of protection thermal threats. The third subdivision is a controlled dynamic experiment to simulate an actual detonation of an ammunition stack and the effects received by a

neighboring stack. All the experiments were recorded with high speed photography and Doppler radar. Temperature data were collected with type K thermocouples.

In the first subdivision, a 454-g steel rectangular slab with sharpened edges was chosen as a simulated fragment threat and is representative of fragments that are produced from a reacted stack of munitions. A black powder charge was used to propel the fragment from a modified gun system (see Figure 8). The fragment velocity was fixed at 60 m/s, and the gun was calibrated to produce repeatable velocities of  $60 \pm 1$  m/s. The velocity data were obtained with the use of Doppler radar (see Figure 9).



Figure 8. Modified Remington 700 Rifle (top) With 40-mm Smooth Bore Fragment Launcher Attachment (bottom).

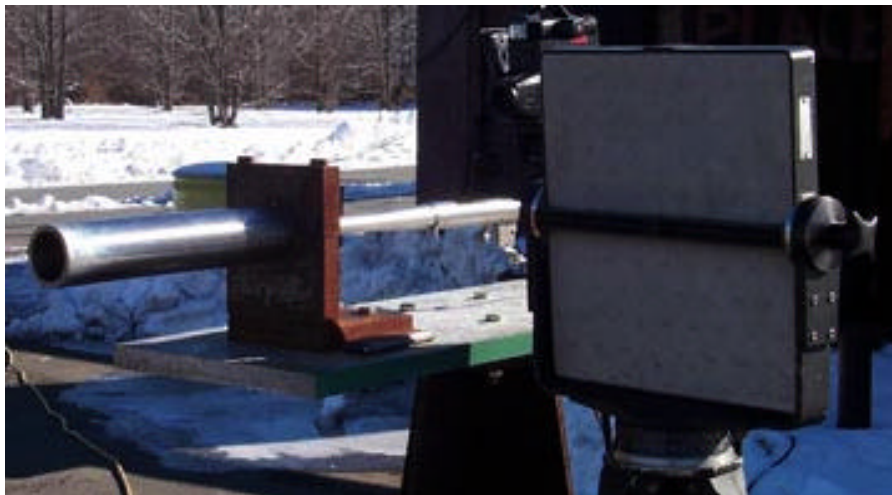


Figure 9. Modified Remington 700 Rifle Assembled and Secured in Firing Bracket Next to Doppler Radar Head.

Five separate blankets consisting of three plies of ceramic fabric sandwiched between four plies of Kevlar<sup>®</sup> were used. A maximum of three fragments was

fired at each sample. If any of the blankets failed, additional plies of Kevlar<sup>®</sup> fabric were added to increase the areal density. If any blanket passed a three-shot experiment, the number of Kevlar<sup>®</sup> plies was reduced until a failure was observed. Plies of Kevlar<sup>®</sup> were added and removed in pairs in order to maintain blanket symmetry. As in Phase 1, successful blankets were evaluated for ballistic properties with a wood backing to simulate a packaged ammunition stack. This will ensure that the blanket provides adequate ballistic protection in unsupported and supported configurations in the field.

The investigation was considered a success if the fragment did not completely penetrate the final ply of Kevlar<sup>®</sup>. Subsequent laboratory experiments determined the size of the damage zone in the ceramic. Flammability studies determined any loss in thermal protection because of impact damage to the ceramic material.

### **2.7.3 Sub-Scale Arena Experiments**

The second subdivision involved the use of live propellant threats to determine the thermal properties of the blankets and their ability to protect stored munitions in case of a fire or explosion. The flame penetration and heat penetration results reduced the number of candidate materials for the required thermal protection by means of a hot gas jet. Several blankets were used to cover live and inert sub-scale acceptor stacks of ammunition. The Phase 1 and Phase 2 ballistic results dictated the final blanket construction in which ceramic layers were sandwiched between a specific number of Kevlar<sup>®</sup> plies.

The blankets were exposed to realistic threats of propellant and burning debris (wood and plastic). Unprotected acceptor stacks of ammunition were exposed to the same threats. The temperature profiles of both the top and bottom surfaces of the blanket as well as the internal crate temperatures were monitored with thermocouples. Based on these results, the number of ceramic plies is adjusted until a satisfactory solution is resolved. The investigation is considered a success if the blanket prevents scorching of the inert acceptors and/or ignition of the live acceptor materials.

The third subdivision subjected larger scale blankets to a simulated dynamic thermal event whereby fragments were propelled at several co-located acceptor stacks covered with prototype blankets. Each sub-scale prototype blanket was subjected to a volley of 0.45-kg projectiles, which produced varying degrees of damage to the blanket. The blankets were then placed on live acceptor stacks and a thermal threat was ignited on top. Any decrease in the flame/heat protection may be attributed to the damage received from fragment impact. The experiment is a success if the blanket prevents severe scorching and ignition of the live acceptor materials.

---

## 3. Results and Discussion

---

### 3.1 Flame Penetration Experiments

In the experiments, a sample surface was exposed to an oxyacetylene flame for a fixed time duration. Samples were mounted and secured on top of a pine wood block by a metal frame or were stapled. Black powder and M9 propellant were placed on top of the sample and between the sample and the pine wood surface. Three different sets of experiments were performed:

1. First Set of Experiments (thick wooden block, metal frame): Samples A to I (see Table 4) and their combinations;
2. Second Set of Experiments (thin wooden block, metal frame): Samples J to O (see Table 3) and their combinations; and
3. Third Set of Experiments (larger sample area, thin wooden block, no metal frame): Samples J, P, Q, and R (see Table 4).

#### 3.1.1 Results from the First Set of Flame Penetration Experiments

In the experiments, samples were mounted on thick pine wood blocks with a metal frame. The sample surface was exposed to an oxyacetylene flame for 3 to 80 seconds. The results are listed in Table 7.

The data in Table 7 indicate that a combination of silica-based samples is more effective in resisting flame penetration. The silica-based sample combinations that appear to be effective are

- Silica cloth (#A)-felt insulation (#B) combination for exposures of less than 60 seconds;
- Silica cloth (#A)-felt insulation (#B-silica fibers)-silica cloth (#A) combination for exposures of less than 80 seconds;
- Siltemp (#E-silica insulation) combination for exposures of less than 40 seconds;
- HTX-1000-9N (#C, silica similar to #A)- Siltemp (#E-silica insulation) combination;
- Silicone-coated silica cloth (#I)- Siltemp (#E-silica insulation) for exposures as long as 30 seconds.

Table 7. Flame Penetration Into a Thick Wood Block With a Smaller Sample

Experiment Number	Sample MST Blanket on Wooden Block Surface	Exposure Duration (seconds)	Wood Behavior
1	No sample, wood surface exposed	3	Charring
2	SiO <sub>2</sub> cloth (#A)	6	Charring
3	Silica cloth (#A) heated to 767 °C	20	Outgassing
4	Silica cloth (#A) over black powdered propellant on wood surface. Propellant exploded in 11 seconds	11	Charring of wood and cloth
5	1/8-in. silica felt (#B)	10	Charring
6	#A/#B layer heated to 700° C	60	Charring- no flaming
7	#A/#B/#A layer heated to 750° C	80	Third layer slightly browned; wood slightly charred
8	Nextel (#D)	6	Burn through- charred wood
9	#D/#D	6	Less severe burn-through than Experiment 8
10	Siltemp (#E)	40	Bottom charred
11	Kevlar /fiber glass (#F) heated to 775° C	5	Burning of wood
12	Kevlar /fiber glass (#F) heated to 700° C	4	Burn through
13	Nomex III aramid (#G)	3	Burn through
14	HTX1000-9N silica (#C) heated to 800° C	15	Burning of wood
15	#C/#E	54	Wood did not char
16	Woven ceramic fibers/Fiberglas (#H)	7	Burn through
17	Silicone-coated silica cloth (#I)	10	Slightly charred
18	#I/#E	30	No char
19	#C/#E + propellant on top of blanket	Propellant ignited immediately	No char
20	#C/#E + propellant between the sample and wooden block	Propellant ignited immediately	Wood and bottom blanket charred
21	#I/#E + propellant on top of blanket	Propellant ignited immediately	No char
22	#I/#E + propellant between the sample and wooden block	Propellant ignited immediately ignition	Wood and bottom blanket charred



### 3.1.2 Results from the Second Set of Flame Penetration Experiments

In the experiments, samples were clamped to thin pine wood blocks with a metal frame. The sample surface was exposed to an oxyacetylene flame for 10 seconds. The results are listed in Table 8.

Table 8. Flame Penetration Into a Thin Wood Block With a Smaller Sample for 10 Seconds' Exposure

Experiment	Sample Combinations	Flame Penetration Into Wood (mm)	Comments
23	Kevlar -glass (#J) over ceramic fiber batting (# N)	13	64-mm square hole on the sample surface
24	Ceramic fiber batting (# N)	9	51- by 64-mm hole on the sample surface
25	Nextel fabric (#K) over ceramic fiber batting (#M)	6	51- by 64-mm hole on the sample surface
26	Nextel fabric (#K) over ceramic fiber batting (#N)	5	51- by 64-mm hole on the sample surface
27	Ceramic fabric (#L)	5	25- by 19-mm hole on the sample surface
28	Ceramic fabric (#L) over ceramic fiber batting (#M)	None	No hole
29	Ceramic fabric (#L) over ceramic fiber batting (# N)	None	No hole
30	Kevlar ballistic blanket (#O)	3	13- by 15-mm hole on the sample surface; 76- by 89-mm wood burned
31	Kevlar ballistic blanket (#O) over ceramic fabric (#L)	None	2-mm penetration into sample
32	Ceramic fabric (#L) with ceramic fiber batting (#M) over Kevlar ballistic blanket (#O)	None	No penetration into sample

Observations in Table 8 show that ceramic-based samples are able to resist flame penetration. Sample combinations that are effective in preventing flame penetration are (a) ceramic fabric (#L) over ceramic fiber batting (#M and #N), (b) Kevlar ballistic blanket (#O) over ceramic fabric (#L), and (c) ceramic fabric (#L) with ceramic fiber batting (#M) over Kevlar ballistic blanket (#O).

### 3.1.3 Results from the Third Set of Flame Penetration Experiments

In the experiments, large, mostly organic fiber-based fabric samples were stapled on thin pine wood blocks. The sample surface was exposed to an oxyacetylene flame for 10 seconds. The results are listed in Table 9.

Table 9. Flame Penetration Into a Thin Wood Block With Larger Samples for 10 Seconds' Exposure

Experiment	Sample Combinations	Flame Penetration Into Wood (mm)	Comments
33	Kevlar -Nomex fabric (# P) on 38-mm thick wooden block	10	Sample burned off
33	Kevlar -glass (#J) on 38-mm thick wooden block	13	25- by 64-mm hole on the sample surface
34	Amatex mineral-coated glass (#Q) on 38-mm thick wooden block	10	64- by 76-mm hole on the sample surface
35	Two layers of Kevlar -glass (#J) on 19-mm thick wooden block	9	13- by 19-mm hole on the sample surface
36	Two layers of (Kevlar -glass (#J) + carbon fiber batting (#R)) on 19-mm thick wooden block	14	13- by 25-mm hole on the sample surface
37	Two layers of (Kevlar -glass (#J) + two layers of carbon fiber batting (#R)) on 19-mm thick wooden block	14	10- x 19-mm hole on the sample surface

The information in the table shows that none of the organic fiber-based fabrics as single or multiple layers prevented flame penetration into wooden block. Thus, it is necessary to use fabrics with a combination of organic and inorganic layers or only inorganic layered fabrics.

### 3.2 Heat Penetration Experiments

In the experiments, a single layer of each sample MST blanket on top of three layers of Kevlar fabric were exposed to an external heat flux of 84 kW/m<sup>2</sup> for 120 seconds. Temperatures versus time measurements were made at the center of the front and back surfaces of the sample and at the center of the back surfaces of the three layers of the Kevlar fabric.

### 3.2.1 Front and Back Temperatures at the Center of the Sample

The measured data for the front and back temperatures at the center of the sample are shown in Figures 4c (No. 8), 5b (No. 3), 6b (No. 4), and in Figures 10 through 15.

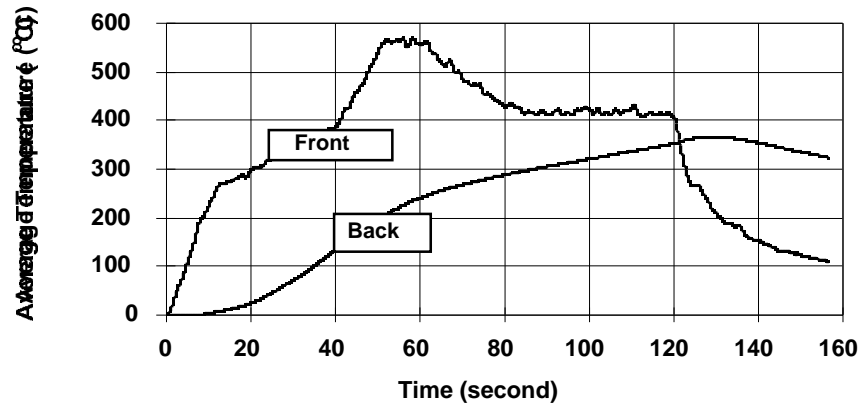


Figure 10. Average Front and Back Surface Temperatures Above Ambient at the Center of 5-mm Thick Sample No. 1. (The black painted surface was exposed to  $84 \text{ kW/m}^2$  for 120 seconds.)

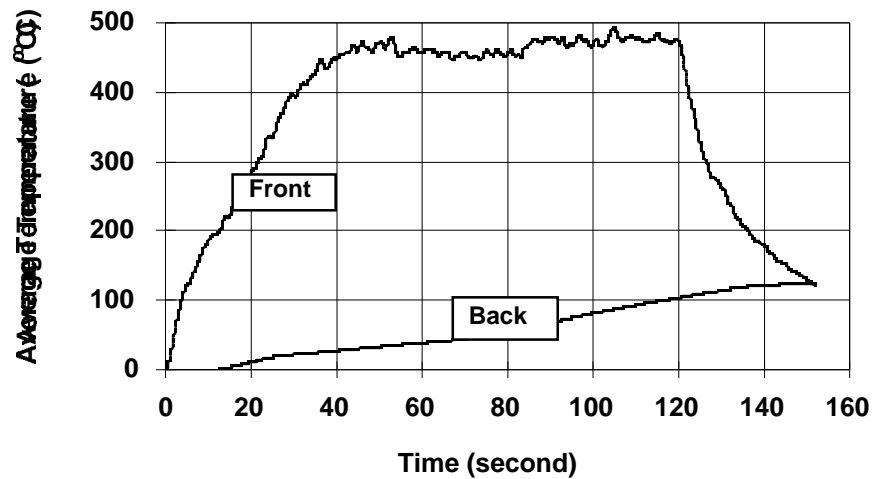


Figure 11. Average Front and Back Surface Temperatures Above Ambient at the Center of 5-mm Thick Sample No. 2. (The black painted surface was exposed to  $84 \text{ kW/m}^2$  for 120 seconds.)

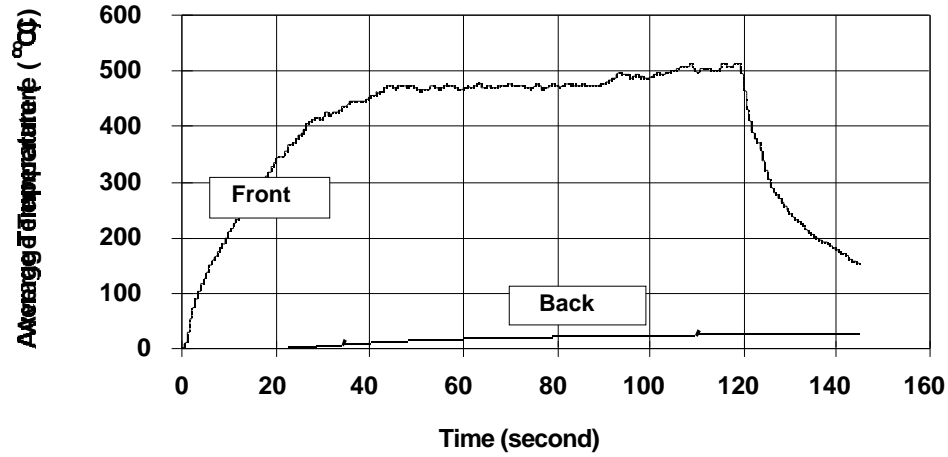


Figure 12. Average Front and Back Surface Temperatures Above Ambient at the Center of 15-mm Thick Sample No. 5. (The black painted surface was exposed to  $84 \text{ kW/m}^2$  for 120 seconds.)

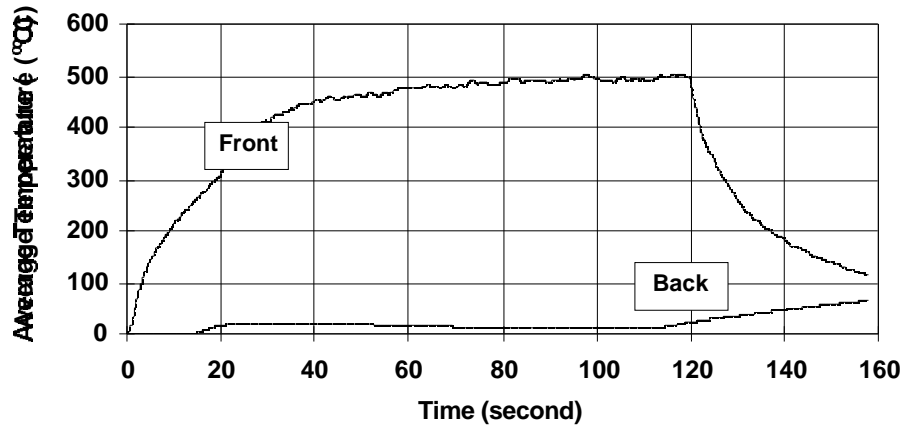


Figure 13. Average Front and Back Surface Temperatures Above Ambient at the Center of 20-mm Thick Sample No. 5. (The black painted surface was exposed to  $84 \text{ kW/m}^2$  for 120 seconds.)

An examination of the front and back surface temperature profiles in the figures indicates that the delay in the rise of back surface temperature depends on the sample thickness and composition. For thin samples (thickness = 5 mm, No. 1, 2, 3, and 4), the rise in the back surface temperature was started between ~20 to 60 seconds. For thicker samples (thickness = 20 to 25 mm, No. 6, 7, 8, and 9), the rise in the back surface temperature started between ~80 and 130 seconds. For Sample No. 5 (15 mm thick), there was a negligible increase in the back surface temperature.

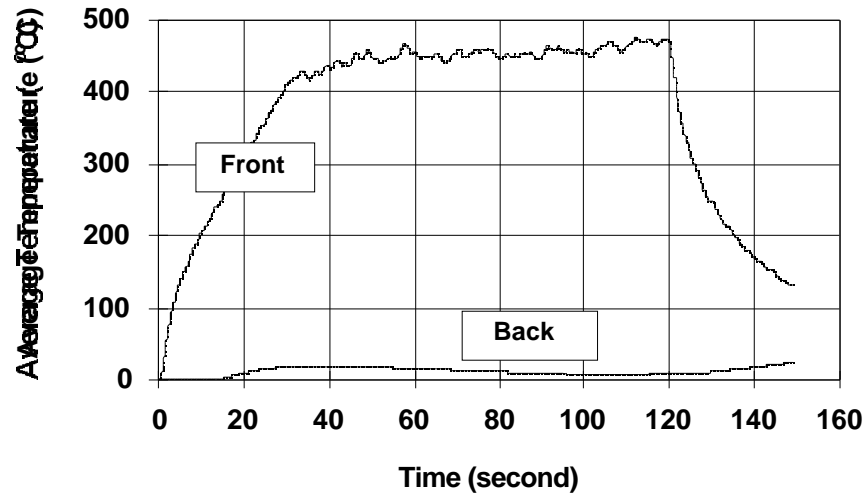


Figure 14. Average Front and Back Surface Temperatures Above Ambient at the Center of 20-mm Thick Sample No. 7. (The black painted surface was exposed to  $84 \text{ kW/m}^2$  for 120 seconds.)

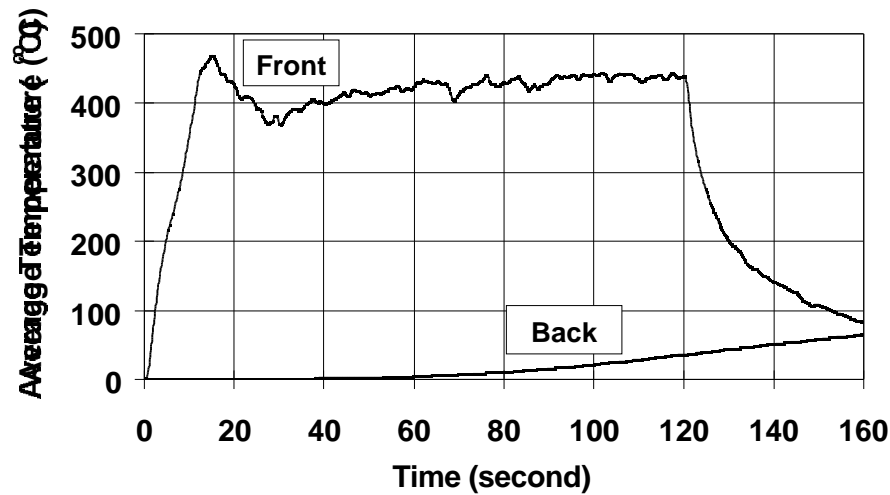


Figure 15. Average Front and Back Surface Temperatures Above Ambient at the Center of 25-mm Thick Sample No. 9. (The black painted surface was exposed to  $84 \text{ kW/m}^2$  for 120 seconds.)

### 3.2.2 Back Surface Temperature of the Sample and Kevlar Fabric Backing

Three layers of organic polymer-based Kevlar fabric were placed behind the sample as a backing. In the experiments, temperatures were measured at the center of the back surface of the sample and each layer of Kevlar fabric as shown in Figure 3. The measured surface temperatures are shown in Figures 16 through 24.

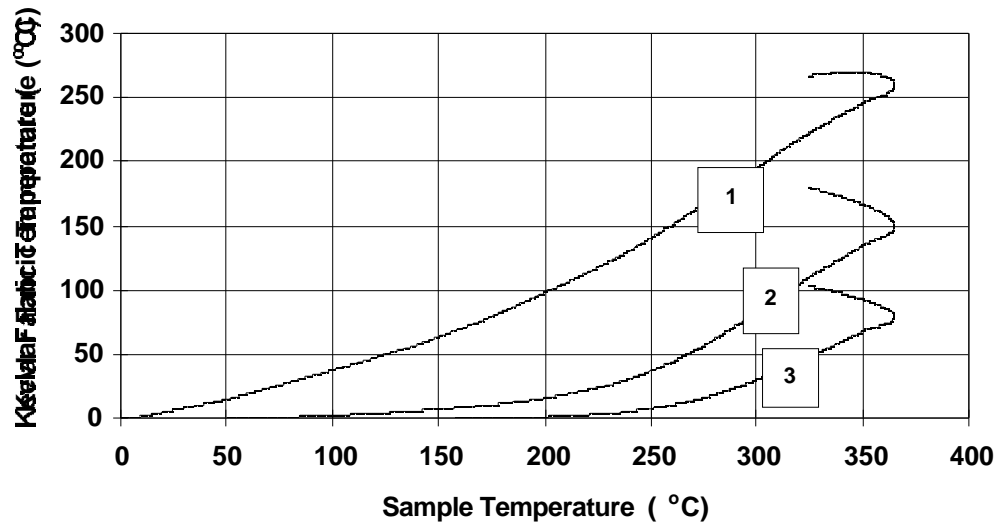


Figure 16. Back Surface Temperature Above Ambient at the Center of 5-mm Thick Sample No. 1 Versus That of the Kevlar Fabric Backing Layers 1, 2, and 3. (The maximum temperature of the front surface of the sample was 400° C.)

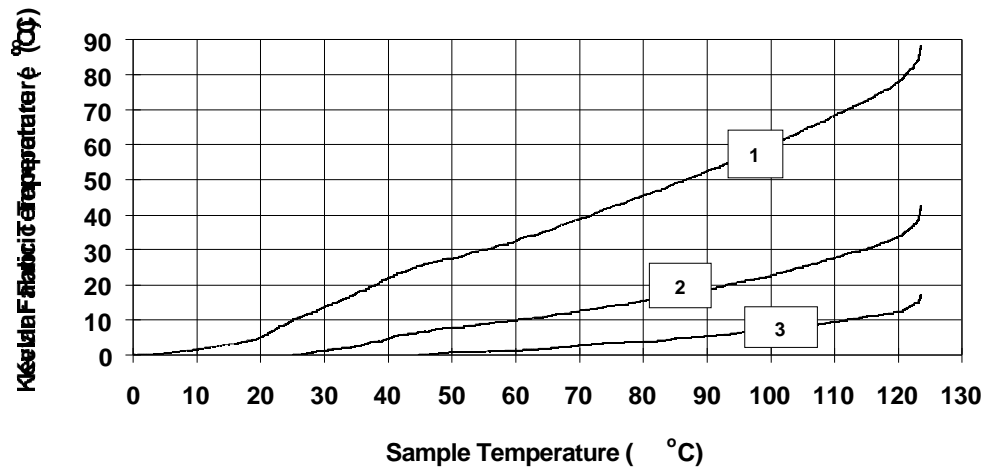


Figure 17. Back Surface Temperature Above Ambient at the Center of 5-mm Thick Sample No. 2 Versus That of the Kevlar Fabric Backing Layers 1, 2, and 3. (The maximum temperature of the front surface of the sample was 440° C.)

The average back surface temperature of each layer of Kevlar fabric was lower than the average back surface temperature of the sample. The average back surface temperature of the bottom third layer of Kevlar fabric was lowest, indicating that Kevlar fabric does provide thermal protection as was found in

the flame penetration experiments (see Table 8, combinations of samples L, M, and O). It is necessary, however, to use at least three layers of Kevlar fabric.

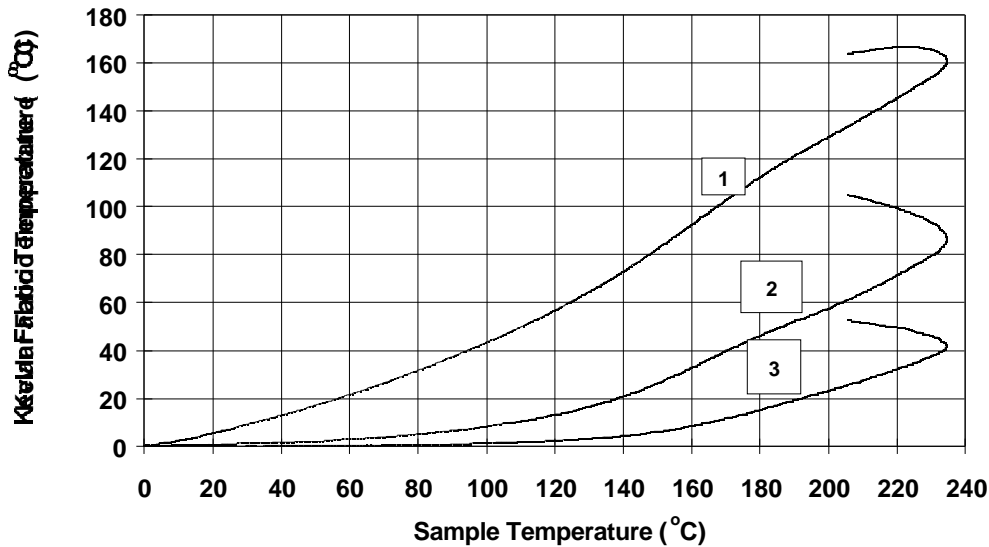


Figure 18. Back Surface Temperature Above Ambient at the Center of Back Surface of 5-mm Thick Sample No. 3 Versus That of the Kevlar Fabric Backing Layers 1, 2, and 3. (The maximum temperature of the front surface of the sample was 550° C.)

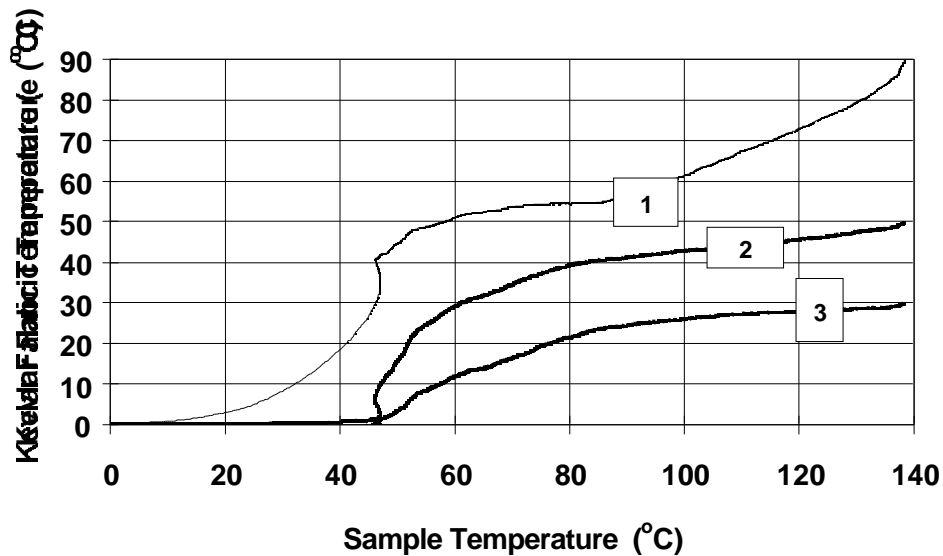


Figure 19. Back Surface Temperature Above Ambient at the Center of 5-mm Thick Sample No. 4 Versus That of the Kevlar Fabric Backing Layers 1, 2, and 3. (The maximum temperature of the front surface of the sample was 490° C.)

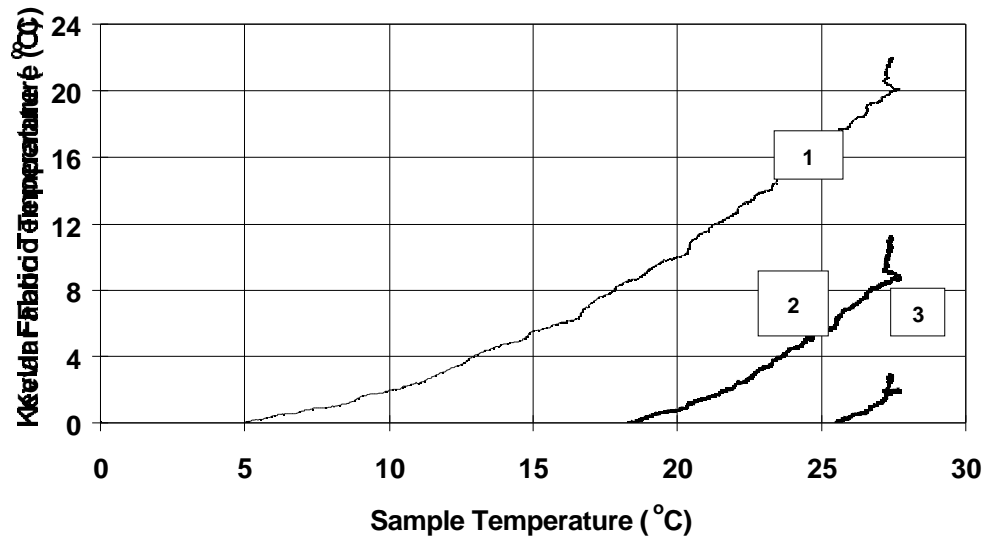


Figure 20. Back Surface Temperature Above Ambient at the Center of 15-mm Thick Sample No. 5 Versus That of the Kevlar Fabric Backing Layers 1, 2, and 3. (The maximum temperature of the front surface of the sample was 450° C.)

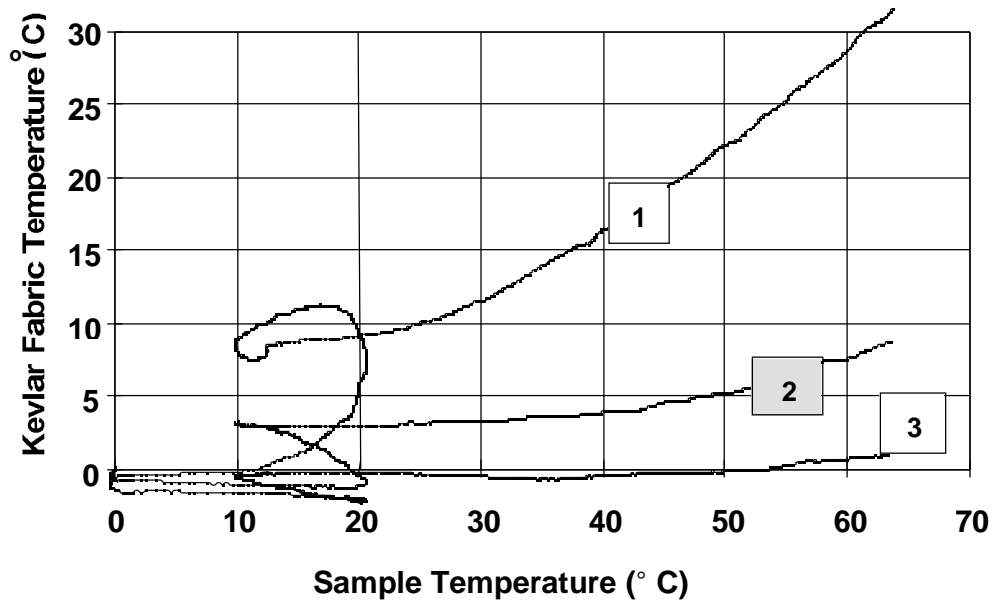


Figure 21. Back Surface Temperature Above Ambient at the Center of 20-mm Thick Sample No. 6 Versus That of the Kevlar Fabric Backing Layers 1, 2, and 3. (The maximum temperature of the front surface of the sample was 475° C.)



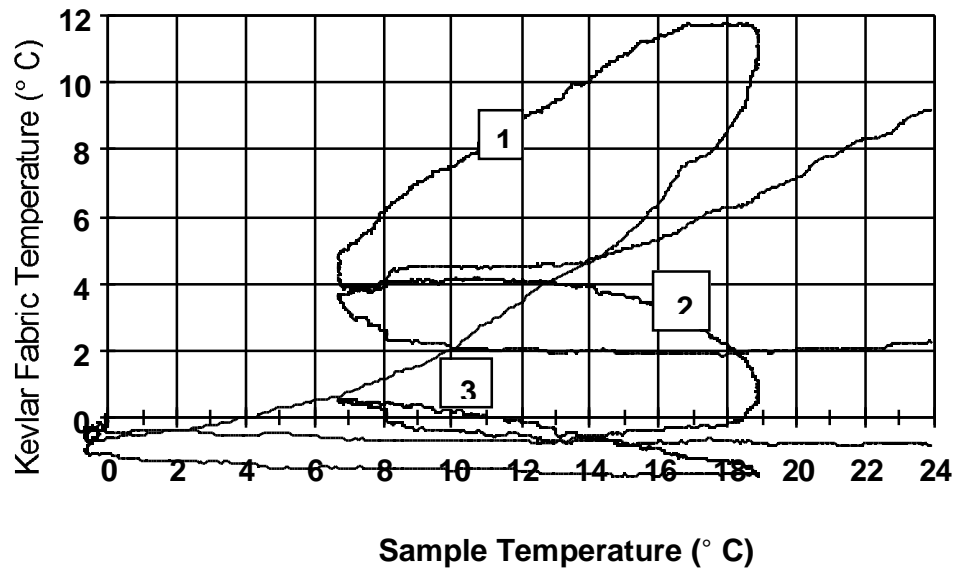


Figure 22. Back Surface Temperature Above Ambient at the Center of 20-mm Thick Sample No. 7 Versus That of the Kevlar Fabric Backing Layers 1, 2, and 3. (The maximum temperature of the front surface of the sample was 430° C.)

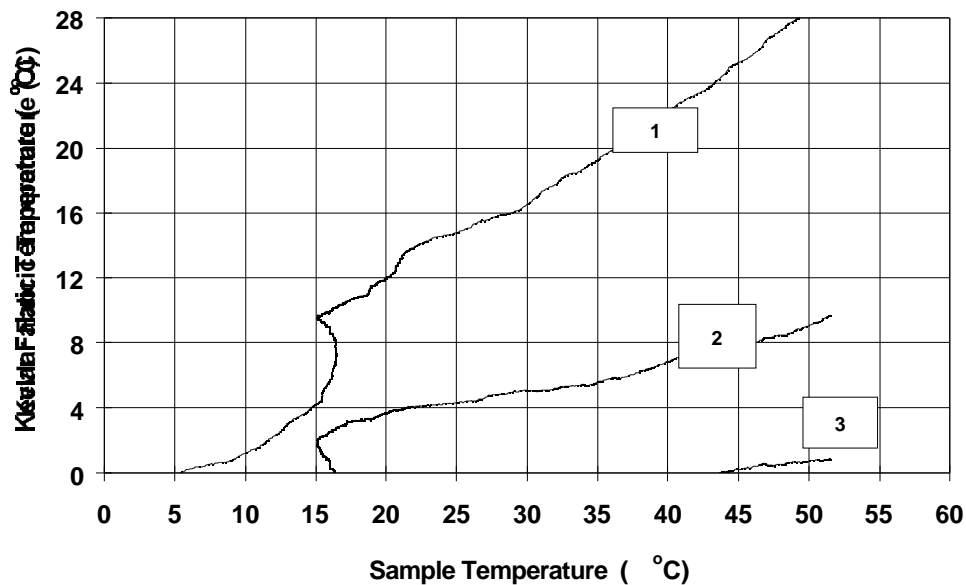


Figure 23. Back Surface Temperature Above Ambient at the Center of 20-mm Thick Sample No. 8 Versus That of the Kevlar Fabric Backing Layers 1, 2, and 3. (The maximum temperature of the front surface of the sample was 444° C.)

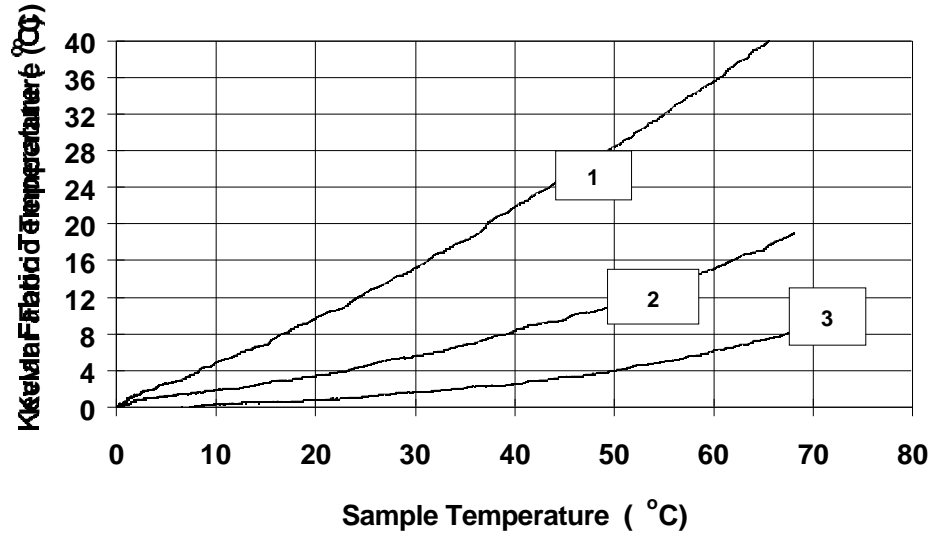


Figure 24. Back Surface Temperature Above Ambient at the Center of 25-mm Thick Sample No. 9 Versus That of the Kevlar Fabric Backing Layers 1, 2, and 3. (The maximum temperature of the front surface of the sample was 440° C.)

Maximum temperatures of the front sample surface and back surface of the third layer of Kevlar fabric are summarized in Table 10. Data in Table 10 indicate that there is a significant decrease in the temperature of the third layer of Kevlar fabric when compared with the front surface temperature of the sample. For a significant reduction in the flame and heat penetration, there is, however, a need to use at least 15- to 25-mm thick layers of inorganic fiber-based fabrics and at least three or more layers of Kevlar fabrics for backing.

### 3.2.3 Resistance to Heat Penetration

As discussed in the background section, effective thermal diffusivity of a fabric system can be considered as a parameter for expressing resistance to heat penetration. The thermal diffusivity of a fabric system can be estimated from the following expression [16]:

$$T_u = T_s \left[ \operatorname{erfc} \left( \frac{x}{2\sqrt{\alpha t}} \right) \right] \quad (1)$$

in which  $T_u$  is the steady state back surface temperature above ambient of the sample (°C),  $T_s$  is the steady state temperature above the ambient of the front (exposed) surface of the sample (°C),  $x$  is the thickness of the sample (mm),  $t$  is the exposure time used in the experiments (120 s), and  $\alpha$  is the effective thermal diffusivity of the sample ( $\text{mm}^2/\text{s}$ ). Effective thermal diffusivity is expressed as  $k/\rho c_p$ , in which  $k$  is the thermal conductivity ( $\text{kW}/\text{m}\cdot\text{K}$ ),  $\rho$  is the density ( $\text{g}/\text{m}^3$ ), and  $c_p$  is the heat capacity ( $\text{kJ}/\text{g}\cdot\text{K}$ ). The expression is used to calculate temperatures inside a material satisfying a thermally thick condition, at various

distances from a hot surface, assuming conduction to be the dominant mode of heat transfer [14].

Table 10. Maximum Temperature of the Front Surface of the Sample and Back Surface of the Third Kevlar Fabric Layer

Sample	Fabric Layers	Thickness (mm)	Maximum Temperature (°C) Front Sample Surface	Back Surface of Third Kevlar Layer
<b>Thin Sample MST Blankets</b>				
1	1000/600 aluminum ; AF – 62 Nextel ; 1000/600 Aluminum	5	400	120; increasing
2	188 CH; 0.13-inch Kaowool paper; Rubberized silica	5	440	40; increasing
3	Zetex 10615-1860; 0.13-inch Kaowool paper; 84 GHS	5	550	70; increasing
4	Ceramic fabric 399C-2 0.13-inch ceramic blanket Ceramic Fabric 399C-2	5	490	50; no increase
<b>Thick Sample MST Blankets</b>				
5	1000/600 aluminum; Copper knit 500; 188 CH	15	450	22; increasing
6	1000/500 stainless steel foil 0.5-in Kaomat ; 188 CH	20	475	< 22; increasing
7	1000/500 OS; 0.5-inch 607 Superwool ; 188 CH	20	430	< 22; no increase
8	1000/800 aluminum; 0.5-inch Kaowool-S ; 188 CH	20	444	< 22; no increase
9	1000/800 stainless steel foil; 0.5-inch 607 Superwool ; 1000/600 aluminum	25	440	30; increasing

The thermal conductivity values for various fabrics selected for the heat penetration experiments are listed in the manufacturers' brochures and range from about  $0.5 \times 10^{-4}$  to  $4 \times 10^{-4}$  kW/m-K. The thermal diffusivity values are generally not listed, except for few fabrics. For example, 3M Company has performed heat conduction experiments with Nextel 312 fabric in a 1093° C

furnace. The temperature inside was measured as a function of time for 1, 3, 6, and 9 layers. Each layer was 0.965 mm. The estimated effective thermal diffusivity values from Equation 1 range from 0.5 mm<sup>2</sup>/s at 120 seconds to 3.2 mm<sup>2</sup>/s at 720 seconds. The effective thermal diffusivity value at 120 seconds is comparable to the values listed in Table 1 for similar types of fabrics.

In the heat penetration experiments,  $T_u$  and  $T_s$  values were measured as functions of time at the center of the sample surfaces. All other information is available to estimate the effective thermal diffusivity of the fabric systems used in the experiments. The effective thermal diffusivity values for the sample MST blankets estimated from the average temperatures measured at the center of the black painted front and back surfaces in the heat penetration experiments are listed in Table 11. The estimated effective thermal diffusivity values for 5-mm thick sample MST blankets agree well with the values listed in Table 1 for similar materials and for values for Nextel 312 fabric.

Table 11. Estimated Effective Thermal Diffusivity  
Values of Sample MST Blankets

Sample Blanket (thickness in mm)	Fabrics and Fibers in Layers of the Sample Blanket	Thermal diffusivity (mm <sup>2</sup> /s)
2 (5 mm)	188 CH; 0.13-inch Kaowool paper; Rubberized silica	0.40
3 (5 mm)	Zetex 10615-1860; 0.13-inch Kaowool paper; 84 GHS	0.64
4 (5 mm)	Ceramic fabric 399C-2 ; 0.13-inch ceramic blanket; Ceramic Fabric 399C-2	0.51
5 (15 mm)	1000/600 aluminum; copper knit 500; 188 CH	2.66
6 (20 mm)	1000/500 stainless steel foil; 0.5-in Kaomat ; 188 CH	4.25
7 (20 mm)	1000/500 OS; 0.5-inch 607 Superwool ; 188 CH	4.13
8 (20 mm)	1000/800 aluminum; 0.5-in Kaowool-S ; 188 CH	5.51
9 (25 mm)	1000/800 stainless steel foil; 0.5-inch 607 Superwool ; 1000/600 aluminum	6.46

The effective thermal diffusivity values of 15- to 25-mm thick sample MST blankets containing metal fibers range between 2.66 and 6.46 mm<sup>2</sup>/s, which are significantly higher than the values of 5-mm thick samples without the metal fibers.

The estimated effective thermal diffusivity values listed in Table 11 can be used to extrapolate the data measured in the heat penetration experiments to higher temperatures and to estimate the back surface temperature of the third layer of the Kevlar fabric backing. In the estimations, the temperatures of the front surface of the sample were assumed to be in the range of 500° to 3000° C, with the actual thickness and estimated effective thermal diffusivity values of the sample MST blankets and heat exposure of the front surface for 10, 30, and 60 seconds. These estimations are listed in Table 12. Note that 15- to 25-mm thick samples resist heat penetration effectively until 3000° C for 60 seconds.

### **3.3 Ballistics and Arena Experiments**

#### **3.3.1 Phase I Ballistics**

Thirty fragment-impact experiments were conducted with the fragments and blanket materials previously described. In most of the experiments, the blankets were secured in a fixture without any backing material. In seven experiments, the blankets were secured in the fixture and backed by a 19-mm thick pinewood panel to simulate a wooden ammunition crate. Other experiments were conducted, backed and unbacked, with a modified right circular cylinder where a pointed tip was fashioned onto the end, thereby concentrating the initial impact force over a smaller area of the blanket.

Two different areal density FFF blankets and three different areal density ARL blankets were evaluated as illustrated in Table 13. The sample identification (ID) describes the type of sample, the number of layers of Kevlar® it contains, and a sequential number to identify the sample. Accordingly, FFF 20-2 is a Federal-Fabrics Fibers sample with 20 plies and is the second sample in the 20-ply series.

Multiple iterations of fragment experiments were performed in order to determine the proper blanket areal density. Based on this phase of ballistic investigation, approximately four to six layers of the ARL, Style #745 Kevlar® 29 were needed to stop a 300-g right circular cylinder fragment. An equivalent areal density of FFF materials failed to stop the fragment. This is primarily because of the loosely woven construction of the fabric. None of the blankets evaluated were able to stop the pointed fragment from penetrating; again, this is because of the woven architecture of the blanket whereby the fragment was able to slide past rather than engage the yarns. In general, this phase of fragment experiments was a worst case scenario in which all fragments impacted “end on” (horizontally) and at a high velocity. An experiment was needed to incorporate a fragment’s natural propensity to tumble in flight and strike a target at several different orientations.

Table 12. Estimated Back Surface Temperatures of the Third Layer of Kevlar Fabric

Sample MST blanket	Temperature Above Ambient (°C)			
	Assumed Front Sample Surface	Third Bottom Kevlar 10-second Exposure $T_{k3}$	Fabric Layer 30-second Exposure $T_{k3}$	60-second Exposure $T_{k3}$
2; $x = 5 \text{ mm};$ $= 0.40 \text{ mm}^2/\text{s}$	1000	11	42	65
	2000	21	85	130
	3000	32	127	195
3; $x = 5 \text{ mm};$ $= 0.64 \text{ mm}^2/\text{s}$	1000	36	93	126
	2000	72	186	251
	3000	108	278	377
4; $x = 5 \text{ mm};$ $= 0.51 \text{ mm}^2/\text{s}$	1000	25	79	113
	2000	51	158	225
	3000	76	237	338
5; $x = 15 \text{ mm};$ $= 2.66 \text{ mm}^2/\text{s}$	1000	4	25	43
	2000	8	50	86
	3000	13	75	129
6; $x = 20 \text{ mm};$ $= 4.25 \text{ mm}^2/\text{s}$	1000	0	3	6
	2000	1	7	12
	3000	6	18	25
7; $x = 20 \text{ mm};$ $= 4.13 \text{ mm}^2/\text{s}$	1000	1	9	15
	2000	2	13	23
	3000	3	26	46
8; $x = 20 \text{ mm};$ $= 5.51 \text{ mm}^2/\text{s}$	1000	1	5	8
	2000	2	10	17
	3000	3	16	25
9; $x = 25 \text{ mm};$ $= 6.46 \text{ mm}^2/\text{s}$	1000	3	24	43
	2000	7	48	87
	3000	10	72	130

Table 13. Areal Density of Kevlar® Ballistic Blankets

	10-ply FFF	20-ply FFF	4-ply ARL	8-ply ARL	13-ply ARL
Average Areal Density ( $\text{kg}/\text{m}^2$ )	1.30	2.64	1.81	3.71	6.16
Standard Deviation	0.01	0.03	0.00	0.01	0.04

### 3.3.2 Phase II Ballistics

As mentioned previously, the fragments used in Phase 2 ballistics were 454-g steel slabs with sharpened edges (see Figure 25). These fragment simulators were launched from a modified Remington 700 rifle with Paradox powder. A sampling of the data is tabulated to show the repeatability of the launching mechanism with the amount of charge used (see Table 14). Once the gun was calibrated, the velocity measurements were no longer recorded. Multiple iterations of fragment experiments were performed in order to determine the proper blanket areal density. Based on this phase of ballistic investigation, four plies of Hexcel-Schwebel Style #745 Kevlar® 29 were sufficient to stop the projectile.

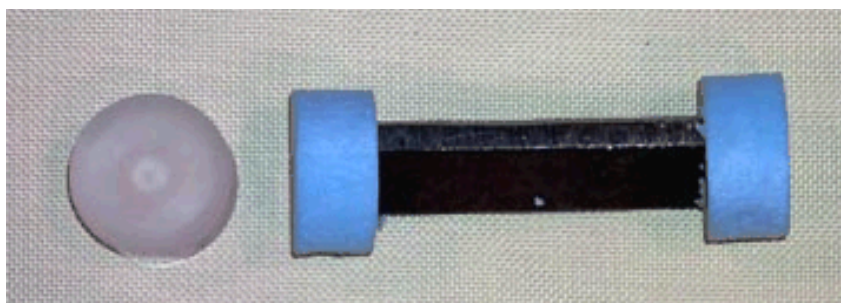


Figure 25. Pusher Plate (left) and 1-lb Steel Fragment With Polymer Foam Sabots Attached on Both Ends. (The pusher plate and sabots are 40 mm in diameter.)

Table 14. Typical Fragment Velocities, Calibration Data of Fragment Launcher, and Penetration Data

Blanket No.	Propellant (grains)	Plies	Velocity (m/s)	Plies Penetrated
1	39	4	64.0	0
2	39	4	60.2	0
3	39	4	57.8	0
4	39	4	59.2	0
5	39	4	62.6	0
6	39	4	59.6	0
7	39	4	64.2	1
8	39	4	59.8	1
9	39	4	58.9	1
10	39	4	59.9	0
11	39	4	58.7	1
12	39	4	60.7	3
13	39	4	59.9	0
14	39	4	63.2	1

Because of fragment impact (see Figure 26) on the target, a number of damaged fibers could easily be observed on the surface, but the investigation was still considered a success since a complete penetration did not occur. A postmortem of the blankets revealed tears in the Kevlar® several layers deep and a small area of damage in the ceramic layers (see Figures 27 and 28). This damage may or may not affect the thermal performance of the blanket.



Figure 26. Blanket Clamped in Frame Impacted by a 454-g Steel Fragment.

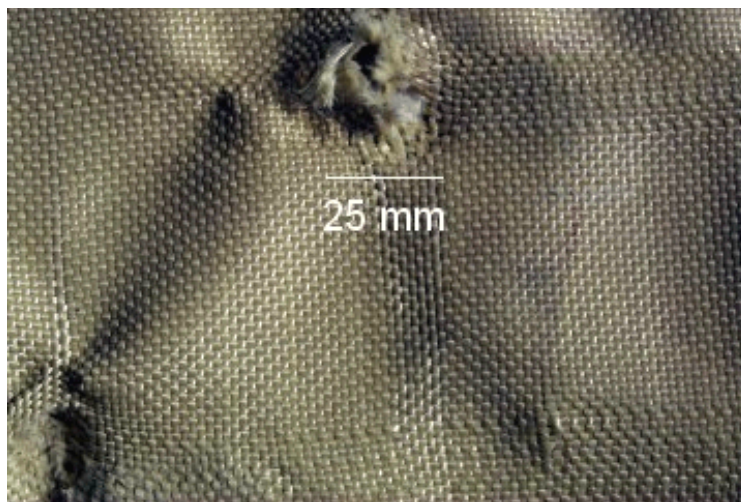


Figure 27. Typical Damage on a Ply of Kevlar as a Result of Impact by a 454-g Steel Fragment.



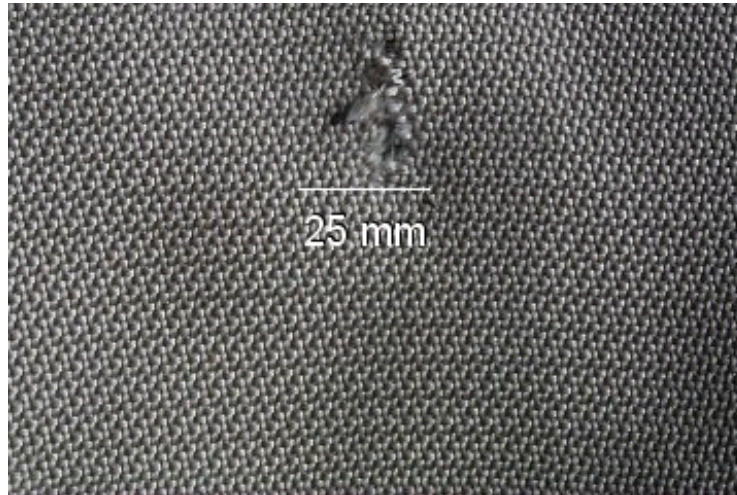


Figure 28. Typical Damage on an Inner Ply of Silica Oxide Fabric as a Result of Impact by a 454-g Steel Fragment.

### 3.3.3 Sub-Scale Arena Experiments

A number of sub-scale arena experiments were performed in order to adequately simulate potential real-life events. The results from both the ballistic fragment penetration experiments and flame/heat resistant experiments were promising.

Static flame experiments were performed with several types of propellant (JA2 and M30) and burning debris. Each represented a fast burning, high temperature threat and a long burning, low temperature threat, respectively. In each experiment, a blanket was used to completely cover a generic ammunition crate (see Figure 29). Thermocouples were placed on top of the blanket, under the blanket, and inside the crate for temperature data collection. Similar experiments were conducted on uncovered inert ammunition crates (see Figure 30).



Figure 29. Fully Assembled Sub-scale Prototype MST Blanket.

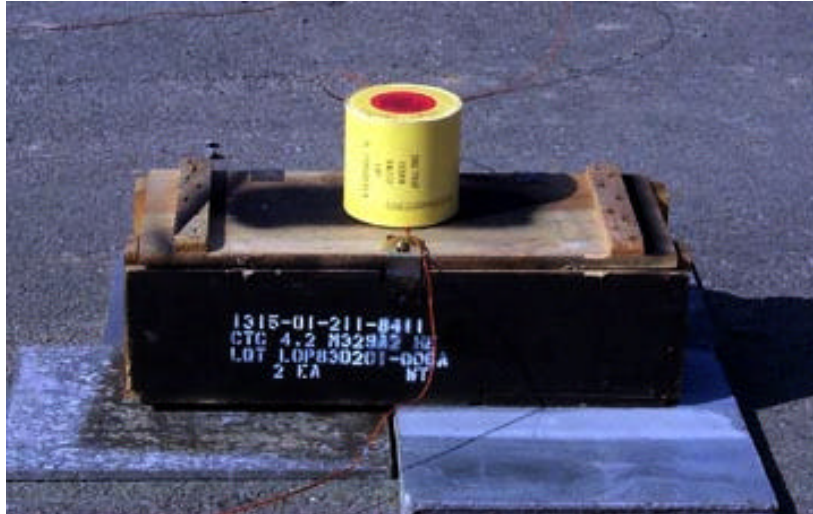


Figure 30. Live Propellant Experiment on an Uncovered Inert Acceptor Ammunition Crate.

Several different amounts of propellant (0.5, 1, 2.5, 5 kg), which represented a short duration, high temperature threat, were placed on the top of the blanket and next to the blanket (see Figure 31). The propellant was ignited with an electric match, while thermocouples and live video were used to capture the event in real time.



Figure 31. Side Burn Propellant Experiment (0.5 kg JA2) on a Covered Inert Acceptor Ammunition Crate.

For the 0.5-kg experiment, the propellant reached a temperature of more than 2000° C and burned for about 5 seconds. The back surface of the blanket and the interior of the wooden crate did not increase in temperature significantly. Similar

results were observed with the 2.5-, 5-, and 10-kg experiments, in which the propellant was ignited, flared, and quickly extinguished, while the back surface of the blanket and the interior of the wooden crate did not increase in temperature substantially. An increase of 50° to 100° C above ambient for short durations were typical values. This was true for both the top-burn and the side-burn experiments. A typical temperature profile (see Figure 32) through the thickness showed a significant difference between the front surface of the blanket and the back surface. The uncovered ammunition crate temperature profile shows a spike in the internal temperature (see Figure 33), which may have easily ignited the contents of a live acceptor. This spike may be attributed to flame penetration between adjacent boards on the crate. A photograph of the blanket (see Figure 34) that covered the acceptor stack shows several layers of scorched nylon and Kevlar®, but the wooden packaging was unperturbed while the uncovered inert crate was totally scorched from the ignited propellant.

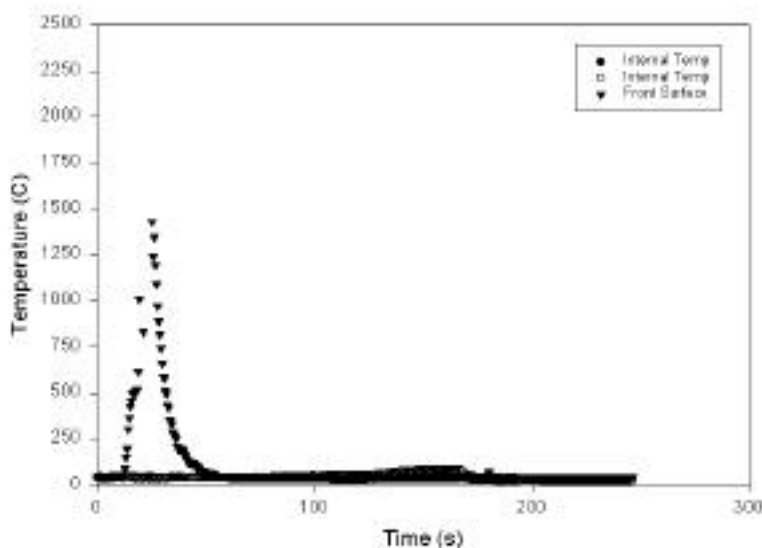


Figure 32. Temperature Profile of a Covered Acceptor Ammunition Crate.

During these static flame experiments, the only time a failure was observed was when the blanket did not completely cover the crate and flames were allowed to penetrate the blanket at a seam and ignite the combustible material underneath. In these instances, the ammunition crate ignited and sustained a burn for an extended length of time. In an actual depot fire, this type of behavior could possibly lead to the sympathetic detonation of neighboring stacks.

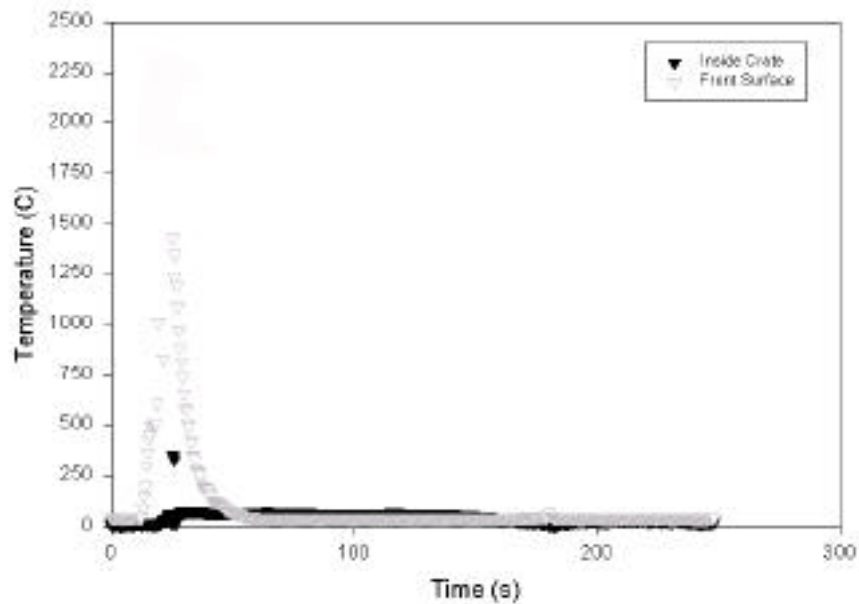


Figure 33. Temperature Profile of an Uncovered Acceptor Ammunition Crate.



Figure 34. Typical Charred Remains of a Top-Burn Live Propellant Experiment.

Bonfire experiments were performed in order to evaluate the effectiveness of these blankets against a lower temperature longer duration thermal threat. Several pounds of JA2 were used to ignite the wood and debris (see Figure 35). Once these items ignited, a blanket-covered ammunition box was placed next to the fire (see Figure 36). The burning embers were then piled on the side of the



blanket and allowed to burn until the flames extinguished (see Figure 36). The temperature profile (see Figure 37) shows that the blanket was effective in retarding heat transfer to the wooden crate for extended periods of time. The one temperature spike observed (see Figure 38) was attributable to the penetration of flames through one of the seams of the blanket. Sandbags were employed in order to prevent any future occurrence. Again, care must be used when these blankets are installed. If the stack is not completely covered by the blanket, flames can easily penetrate and cause a catastrophic failure.



Figure 35. Setup of Bonfire Experiment Before Ignition.



Figure 36. Bonfire Experiment Several Minutes After Ignition.



Figure 37. Bonfire Experiment After the Flames Self-Extinguished.

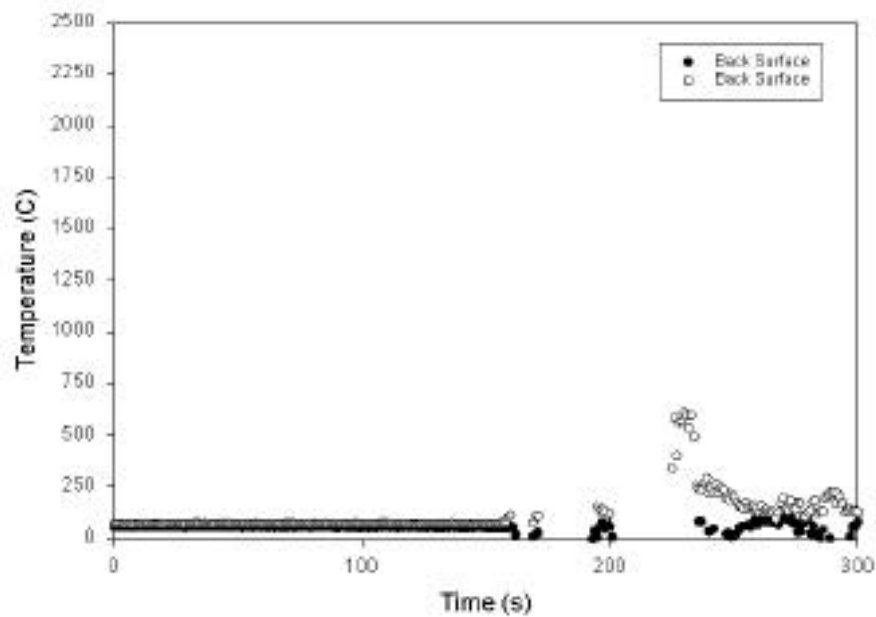


Figure 38. Temperature Profile of a Bonfire Experiment.

Another arena experiment, which evaluated the blanket in extreme temperatures, simulated the ignition of a tubular storage container of 155-mm artillery uni-charge packages. Four uni-charge packages were placed in a 155-mm steel tube, which was blocked at one end with a steel plate (see

Figure 39). The blanket-covered target was placed approximately 1 m from the opening of the tube to ensure direct contact with the hot gas jet (see Figure 40).



Figure 39. Setup of Uni-charge Experiment, in Which Four Uni-charge Packages Were Placed Inside the Steel Tube.



Figure 40. Setup of Uni-charge Experiment, Showing Stand-off Distance.

The first uni-charge was ignited with an electric match and the other three successively auto-ignited during the experiment. The blanket was subjected to a tremendous gas jet for approximately 2 minutes. The flames ablated the protective outer cover, and several layers of Kevlar<sup>®</sup> (the ceramic inner layers) were also heavily damaged (see Figure 41) during the event.





Figure 41. Results From a Uni-charge Experiment.

The back surface of the blanket was still intact (see Figure 42), and the temperature profile illustrates the blanket's ability to protect stored munitions from a severe thermal threat (see Figure 43). The charred edge is where some flames were able to breach the blanket, which resulted in a temperature spike on one of the thermocouple channels. Again, the temperature spike was attributable to flame migration through a seam and not to a failure from a complete burn-through of the blanket. If this blanket had been made entirely of Kevlar<sup>®</sup>, as in the BPS, this experiment would have surely been a failure with a total burn-through the thickness of the blanket. The inorganic layers of ceramic fabric provided the required high performance for an aggressive threat such as this.



Figure 42. Back Surface of a Blanket Subjected to a Hot Gas Jet Emitted From Four Uni-charge Packages.



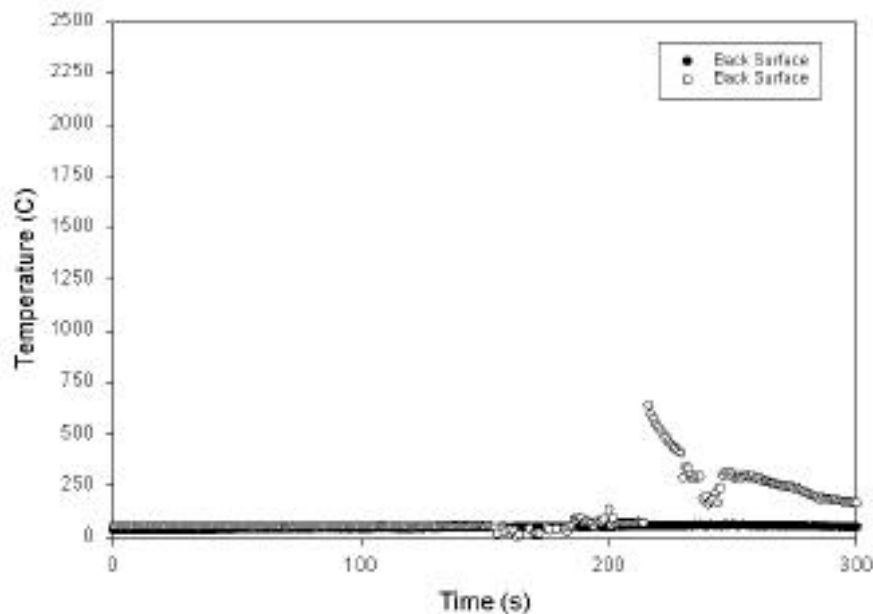


Figure 43. Temperature Profile of the Back Surface of a Blanket From a Uni-charge Experiment.

In the next arena experiment, the sub-scale blankets were subjected to a volley of six 454-g fragments in which several small tears in the blanket that were similar to previously illustrated tears were observed (see Figures 27 and 28). These blankets were then placed on acceptor stacks, which consisted of inert wooden packaging material and live, loose uni-charge packages (see Figures 44 and 45). Generally, the outer layer of nylon and the first layer of Kevlar® were charred (see Figure 46) and the back surface increased about 75° C above ambient. The two curves in Figures 47 and 48 represent experiments in which two different types of blankets were placed on the wooden packaging material. The curves illustrate the blanket's ability to protect the wood packaging and ammunition from heat and flame. As expected, the more insulation present (i.e., layers of Kevlar®), the lower the back surface temperature.

There were no visible signs that flames were able to penetrate the blanket, although holes were present. This may be attributed to the shifting of individual layers to cover holes in neighboring plies. This phenomenon eliminates a direct path for the fire and heat to penetrate.



Figure 44. Uni-charge Placed on Top of a Covered Inert Acceptor Before Ignition.



Figure 45. Uni-charge Placed on Top of a Covered Live (Uni-charge) Acceptor Before Ignition.



Figure 46. Typical Results From the Ignition of a Uni-charge on Top of an MST Blanket.

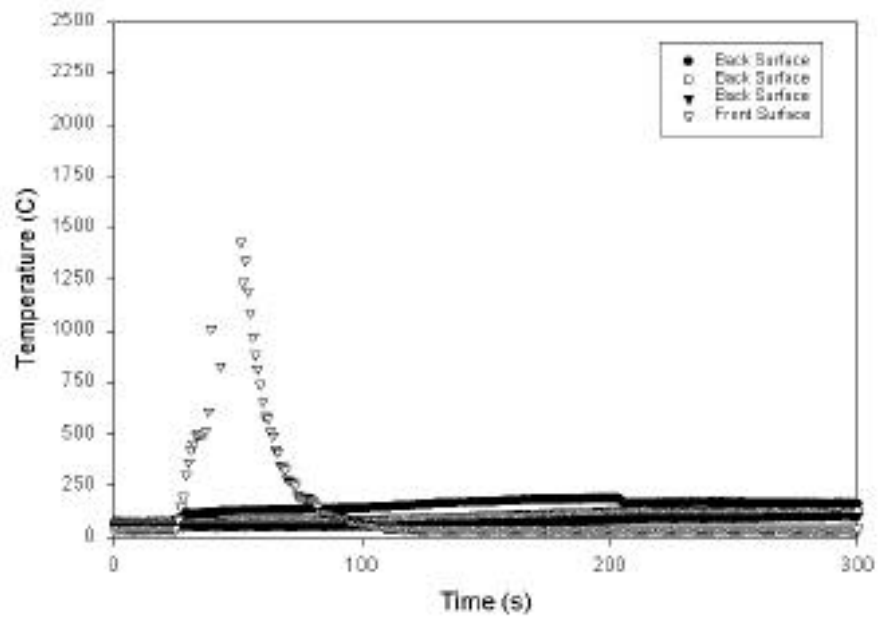


Figure 47. Temperature Profile Results From the Ignition of a Uni-charge on Top of an Undamaged MST Blanket (four plies of Kevlar®).

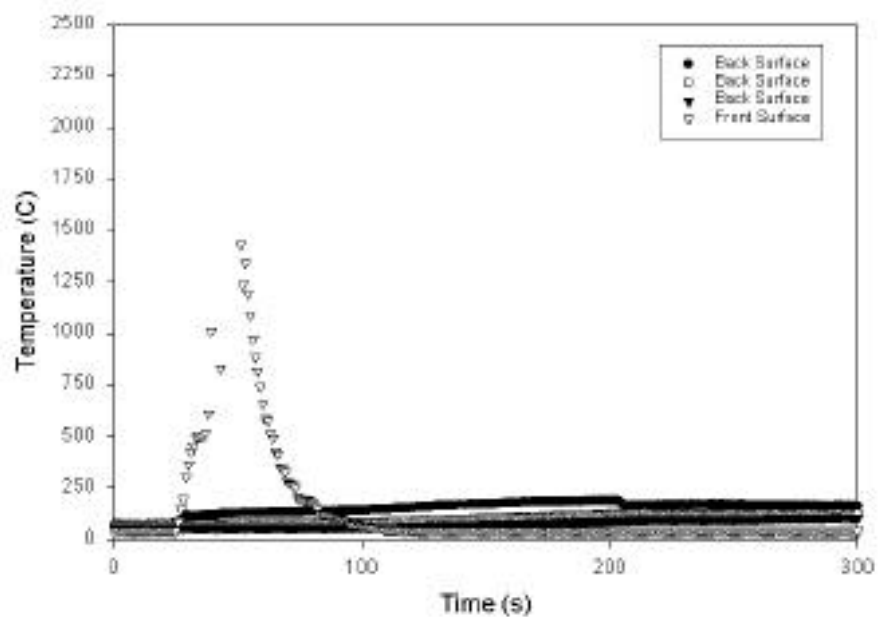


Figure 48. Temperature Profile Results From the Ignition of a Uni-charge on Top of an Undamaged MST Blanket (five plies of Kevlar®).

The next two curves (see Figures 49 and 50) are from experiments in which the damaged blankets were placed on top of a live acceptor and a uni-charge was ignited on top of the blanket. The uni-charge was positioned directly above the acceptor and temperature data were collected (see Figure 51). Again, a small increase in the back surface temperature was observed but the blankets appear to have been effective in preventing ignition of the acceptor propellant.

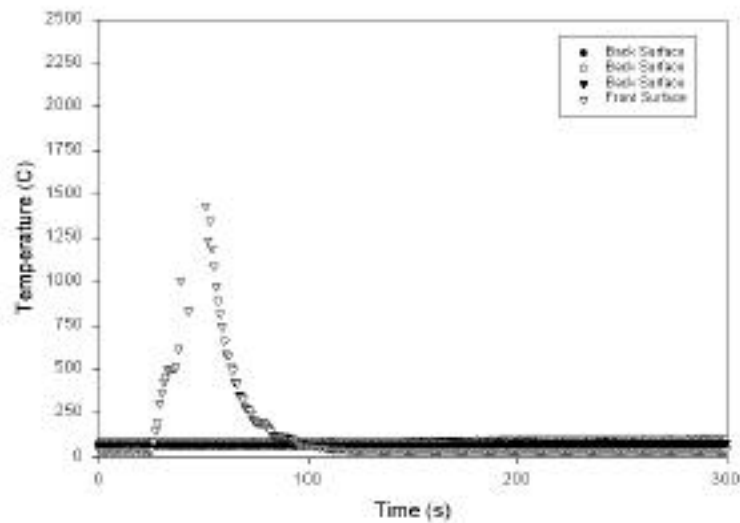


Figure 49. Temperature Profile of a Live Acceptor Under a Torn Blanket With a Uni-charge Ignited on Top (four layers of Kevlar®).

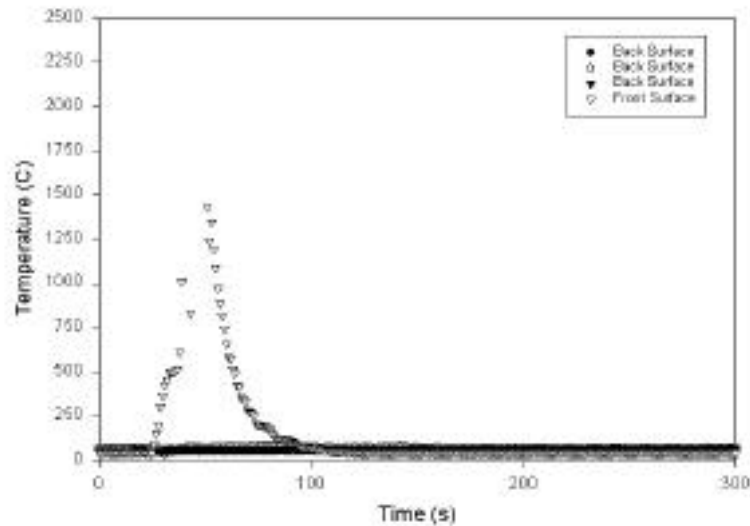


Figure 50. Temperature Profile of a Live Acceptor Under a Torn Blanket With a Uni-charge Ignited on Top (five layers of Kevlar®).



Figure 51. Instrumented Acceptor Stack of Ammunition After Several Experiments.

### 3.4 Blanket Design Considerations

A manufacturing effort needs to address several issues, including (a) the formation of a seamless blanket that prevents flame/heat penetration and (b) the long-term durability of some of the ceramic materials. Seamless construction will improve the effectiveness since the flame cannot penetrate the seam between adjacent segments. Improvements in the stitching process may reduce the fracture of the ceramic felt material along the stitched locations of the blanket. This felt fracture (see Figure 52) might be detrimental to the thermal performance of the blanket over time because of rough handling.

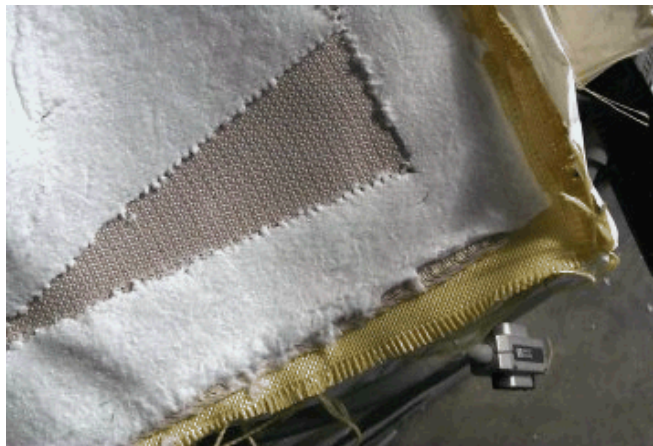


Figure 52. The Effect of Stitching on the Brittle Ceramic Felt Material.

These blankets were configured so that they provided optimal protection from ballistic and thermal threats. A composite construction was chosen because of the unique requirements of the blanket (see Figure 53). The number of layers of Kevlar® was established, based on the low velocity ballistic experiments. The number of layers of ceramic fabric was dictated by the results of the heat/flame penetration experiments.

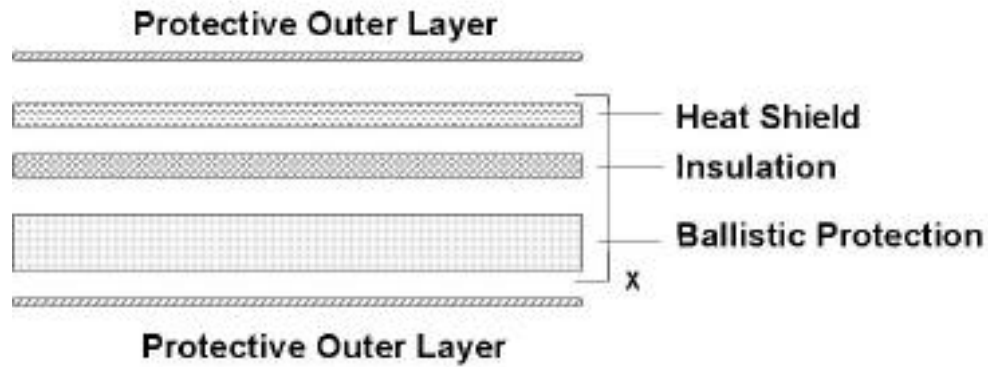


Figure 53. Composite Sandwich Schematic Showing Different Layers of Material.

From the total number of layers in the blanket, an areal density can be determined. Based on areal density, the blanket cost and appropriate weight per section can be established. Table 15 illustrates some sample calculations to determine some of these parameters which compare the MST blanket, a BPS blanket, and a BPS with ceramic material added to the system.

Based on the requirements for the MST blanket, it is apparent that the BPS cannot be substituted for the MST blanket because of its poor flame penetration properties, nor could the ceramic material be added to the BPS in its current configuration because of cost and weight issues.

---

## 4. Conclusions

---

### 4.1 Flammability

- Literature information and flame and heat penetration data from this study suggest that the use of a combination of commercially available inorganic (alumina, silica, and ceramic) and organic (Kevlar ) fiber-based fabrics in multiple layers is effective in enhancing the resistance of the fabric systems to flame and heat penetration.

Table 15. Weight and Cost Estimates for MST Blanket, BPS Blanket,  
and a BPS-Ceramic Hybrid Solution

Material	Area Covered (m <sup>2</sup> )	Weight per Ply (kg/m <sup>2</sup> )	No. Plies	Weight (kg/m <sup>2</sup> )	Cost/ply (\$/m <sup>2</sup> )	Total Weight (kg)	Total Cost (\$)	Ply Thickness (mm)	Total Thickness (mm)
<b>MST Blanket</b>									
Kevlar 29	46.50	0.44	4	1.76	19.78	81.82	3680	0.64	2.54
Ceramic Fabric	46.50	0.64	2	1.27	27.96	59.09	2600	0.64	1.27
Ceramic Felt	46.50	0.73	1	0.73	13.98	34.09	650	3.18	3.175
Cordura Cover	46.50	0.24	2	0.49	4.95	22.73	460	0.38	0.762
Labor/Misc.			9	4.25	66.67	197.73	7390		7.747
<b>BPS</b>									
Kevlar 29	46.50	0.44	13	5.72	19.78	265.91	11960	0.64	8.255
Ceramic Fabric	46.50	0.64	0	0.00	27.96	0.00	0	0.64	0
Ceramic Felt	46.50	0.73	0	0.00	13.98	0.00	0	3.18	0
Cordura Cover	46.50	0.24	2	0.49	4.95	22.73	460	0.38	0.762
Labor/Misc.			15	6.21	66.67	288.64	12420		9.017
<b>BPS+Ceramic</b>									
Kevlar 29	46.50	0.44	13	5.72	19.78	265.91	11960	0.64	8.255
Ceramic Fabric	46.50	0.64	2	1.27	27.96	59.09	2600	0.64	1.27
Ceramic Felt	46.50	0.73	1	0.73	13.98	34.09	650	3.18	3.175
Cordura Cover	46.50	0.24	2	0.49	4.95	22.73	460	0.38	0.762
Labor/Misc.			18	8.21	66.67	381.82	15670		13.462

- Several combinations of the inorganic fiber-based fabrics with three layers of Kevlar® fabric backing were used as sample MST blankets. Data from the study suggest that to prevent heating of the back surface of the sample MST blanket, the front layers of the inorganic fiber-based fabrics need to be greater than 5 mm in thickness and at least three layers of Kevlar® fabric layers need to be used as backing layers.
- Effective thermal diffusivity values of sample MST blankets provide a useful parameter to estimate their effectiveness in preventing flame and heat penetration in the back of the sample MST blankets.
- A procedure has been developed to obtain effective thermal diffusivity of the sample MST blankets from the measured average steady state temperatures at the center of the front and back surfaces, thickness, and exposure time duration. The effective thermal diffusivity values of the sample MST blankets are in good agreement with the literature values for generically similar fabric systems.

## **4.2 Phase 1 Ballistics**

- The shape of the fragment and its orientation at impact have a large effect on the degree of blanket penetration.
- For approximately the same areal density, the ARL style #745 Kevlar® tightly woven blanket is more effective for stopping fragments than the FFF 1500-denier, loosely woven material. Approximately four to six layers are required to prevent penetration of a flat-faced, cylindrical steel fragment that weighs 0.3 kg, is 170 mm long and 17 mm in diameter, and is traveling at a velocity of 146 m/s.
- A modified conical nosed fragment penetrated all ARL and FFF blankets studied.
- The addition of wood panels behind the blanket gave mixed results for fragment penetration protection.

## **4.3 Phase 2 Ballistics**

- Four layers of Kevlar® style #745 were sufficient to prevent a 454-g rectangular slab fragment traveling at 60 m/s from penetrating an ammunition stack in both supported and unsupported configurations. Therefore, the addition of a wood panel behind the blanket did not affect the performance of the blanket.
- Small holes were observed in both the Kevlar® and the ceramic fabric, but complete penetration did not occur.



#### **4.4 Sub-Scale Arena Experiments**

- Prototype blankets consisting of four or five layers of Kevlar 29<sup>®</sup>, two layers of nylon, and three layers of silica felt/fabric passed a variety of fragment penetration experiments and heat/flame experiments. The specifications for each layer are listed in Table 15.
- The materials evaluated should protect stored ammunition from low velocity fragments and assorted thermal threats, provided that the blanket is manufactured correctly, assembled correctly, and used in concert with earthen barricades.

#### **4.5 Issues and Concerns**

- One issue that needs to be addressed is an effective way to ensure that the blanket totally covers the stored ammunition. The materials evaluated in this research effort are extremely effective in preventing the ignition and detonation of an ammunition stack, but if a firebrand is able to penetrate a seam or migrate under a pallet, the blanket will not be effective. More work needs to be done to make the individual segments perform as a single seamless unit.
- The effect of stitching on the fabrics needs to be addressed in a manufacturing effort. The felt ceramic is an effective insulator but is brittle and may fracture during rough handling and blanket fabrication. Other materials may be substituted, which combine the same ceramic felt material in a flexible organic matrix but at an increased weight.
- Another recurring issue with the designs studied was the continued burning/smoldering of the nylon protective outer cover. Although it is advertised as a flame-retardant material, it is not completely flame resistant. This material ignites at a higher temperature than non-flame-retardant nylons, but once it is ignited, it may continue to burn slowly. A silicone-coated fiberglass, which was evaluated in this study but rejected because of weight and cost issues, may be an appropriate substitution for this protective outer cover.

---

## References

---

- Frey, R.B., and J. Starkenberg, "The Vulnerability of Ammunition Stacks to Small Fragments," ARL-TR-2030, U.S. Army Research Laboratory, Aberdeen Proving Ground, MD, August 1999.
- Finnerty, A.E., "Fire Tests of Ammunition in Wooden Boxes," BRL-MR-3936, Ballistics Research Laboratory, Aberdeen Proving Ground, MD, August 1991.
- Shanley, L.A., B.L. Slaten, P. Shanley, R. Broughton, D. Hall, and M. Baginski, "Thermal Properties of Novel Carbonaceous Fiber Battings," Journal of Fire Sciences, 12, 238, 1994.
- Myers, R.E., and E. Licursi, "Inorganic Glass-Forming Systems as Intumescent Flame Retardant for Organic Polymers," Journal of Fire Sciences, 3, 415, 1985.
- Lem, K.W., Y.D. Kwon, H.B. Chin, H.L. Li, and D.C. Prevorsek, "Spectra Composite That Withstands Torch Flame Test," Journal of Fire Sciences, 1, 147, 1993.
- Saad, M.A., and R.L. Altman, "Thermal Protection Studies of Plastic Films and Fibrous Materials," Journal of Fire Sciences, 6, 250, 1988.
- Kourtides, D.A., W.C. Pitts, M. Araujo, and R.S. Zimmerman, "High Temperature Properties of Ceramic Fibers and Insulations for Thermal Protection of Atmospheric Entry and Hypersonic Cruise Vehicles," Journal of Fire Sciences, 6, 313, 1988.
- Damant, G.H., "Use of Barriers and Fire Blocking Layers to Comply with Full Scale Fire tests for Furnishings," Journal of Fire Sciences, 14, 3, 1996.
- Polymer News, 8, 177, 1996.
- Newtex, 8050 Victor-Mendon Road, Victor, NY.
- Thermal Ceramics, P.O. Box 923, Augusta, GA.
- Christy Refractories Company, 4641 McRee, St. Louis, MO.
- 3M Ceramic Materials Department, 3M Center Building St. Paul, MN.
- RM Engineered Products Inc, 4854 O'Hear Avenue, North Charleston, SC.
- Marker, T.R., "Full-Scale Test Evaluation of Aircraft Fuel Fire Burn-through Resistance Improvements," Final Report DOT/FAA/AR-98/52, Office of Aviation Research, Washington, DC, July 1999. National Technical Information Service, Springfield, VA 22161.
- Carslaw, H.S., and J.C. Jaeger, Conduction of Heat in Solids, Second Edition, Oxford at the Clarendon Press, Oxford, England, 1959.
- Dupont Kevlar® Literature H-77877 1998.

Allied Signal Spectra Shield Literature AS-PF-PS9A 1999

Mackiewicz, J.F., "Development of Protective Ballistic Covers," ARL-TR-86, U.S. Army Research Laboratory, Aberdeen Proving Ground, MD, February 1993.

Hexcel-Schwebel High Performance Fabric Literature 1997.

Natick SBCCOM Ballistic Protective System Fact Sheet March 15 2000.

Boyle, V.M., A.L. Bines, and W.B. Sunderland, "Munitions Survivability Technology: A Comparison of Two Different Blanket Designs for Protecting Against an Indirect Fragment Threat," ARL-TR-2122, U.S. Army Research Laboratory, Aberdeen Proving Ground, MD, Nov 1999.

NO. OF  
COPIES    ORGANIZATION

1 ADMINISTRATOR  
DEFENSE TECHNICAL INFO CTR  
ATTN DTIC OCA  
8725 JOHN J KINGMAN RD  
STE 0944  
FT BELVOIR VA 22060-6218

1 DIRECTOR  
US ARMY RSCH LABORATORY  
ATTN AMSRL CI AI R REC MGMT  
2800 POWDER MILL RD  
ADELPHI MD 20783-1197

1 DIRECTOR  
US ARMY RSCH LABORATORY  
ATTN AMSRL CI LL TECH LIB  
2800 POWDER MILL RD  
ADELPHI MD 207830-1197

1 DIRECTOR  
US ARMY RSCH LABORATORY  
ATTN AMSRL D D SMITH  
2800 POWDER MILL RD  
ADELPHI MD 20783-1197

1 OSD  
ATTN OUSD(A&T)/ODDDR&E(R)  
ATTN R J TREW  
THE PENTAGON  
WASHINGTON DC 20310-0460

1 INST FOR ADVNCD TCHNLGY  
THE UNIV OF TEXAS AT AUSTIN  
PO BOX 202797  
AUSTIN TX 78720-2797

1 NAV SURFACE WARFARE CTR  
ATTN CODE B07 J PENNELLA  
17320 DAHLGREN RD  
BLDG 1470 RM 1101  
DAHLGREN VA 22448-5100

1 DARPA  
3701 N FAIRFAX DR  
ARLINGTON VA 22203-1714

NO. OF  
COPIES    ORGANIZATION

1 US MILITARY ACADEMY  
MATHEMATICAL SCIENCES CTR  
OF EXCELLENCE  
DEPT OF MATH SCIENCES  
ATTN MDN A MAJ HUBER  
THAYER HALL  
WEST POINT NY 10996-1786

10 ASCO LOGISTICS R&D ACTVTY  
ATTN AMSTA AR ASL D SCARBOROUGH  
BLDG 455  
PICATINNY ARSENAL NJ 07806-5000

ABERDEEN PROVING GROUND

2 DIRECTOR  
US ARMY RSCH LABORATORY  
ATTN AMSRL CI LP (TECH LIB)  
BLDG 305 APG AA

20 DIRECTOR  
US ARMY RSCH LABORATORY  
ATTN AMSRL WM MA W CHIN (10)  
T MULKERN (10 CYS)  
BLDG 4600

3 DIRECTOR  
US ARMY RSCH LABORATORY  
ATTN AMSRL WM TB R FREY  
R LOTTERO  
J STARKENBERG  
BLDG 309

1 DIRECTOR  
US ARMY RSCH LABORATORY  
ATTN AMSRL WM TB  
W HILLSTROM  
BLDG 1119B

ABSTRACT ONLY

1 DIRECTOR  
US ARMY RSCH LABORATORY  
ATTN AMSRL CI AP TECH PUB BR  
2800 POWDER MILL RD  
ADELPHI MD 20783-1197

1 DPTY CG FOR RDA  
US ARMY MATERIEL CMD  
ATTN AMCRDA  
5001 EISENHOWER AVE  
ALEXANDRIA VA 22333-0001

INTENTIONALLY LEFT BLANK

Cerachem , Cerawool , Kaomat , and Kaowool are registered trademarks of Thermal Ceramics.

Curlon is a registered trademark of Orcon Corporation.

Dacron , Kapton , Kevlar , Nomex , and Tedlar are registered trademarks of E.I. DuPont de Nemours & Co., Inc.

Duraback<sup>TM</sup> is a trademark of Unifax Corporation.

Durablanket is a registered trademark of Unifax Corporation.

Dyneema is a registered trademark of Toyobo Japan.

Fluorel<sup>TM</sup> is a trademark of Fluorel SA.

Kao-Tex<sup>TM</sup> is a trademark of Thermal Ceramics.

Microsoft is a registered trademark of Microsoft Corporation.

Nextel<sup>TM</sup> is a trademark of 3M Corporation.

Quartzel is a registered trademark of Saint-Gobain Industrial Ceramics.

Siltemp is a registered trademark of Amatek Chemical Products.

Solimide is a registered trademark of Inspec Foams.

Spectra is a registered trademark of Honeywell.

Superwool is a registered trademark of Morgan Materials Technology Ltd, England

Twaron is a registered trademark of Acordis.

Windows<sup>TM</sup> is a trademark of Microsoft Corporation.

Zetex and Zetex Plus are registered trademarks of Newtex Industries, Inc.

The findings in this report are not to be construed as an official Department of the Army position unless so designated by other authorized documents.

Citation of manufacturer's or trade names does not constitute an official endorsement or approval of the use thereof.

Destroy this report when it is no longer needed. Do not return it to the originator.

Cerachem , Cerawool , Kaomat , and Kaowool are registered trademarks of Thermal Ceramics.

Curlon is a registered trademark of Orcon Corporation.

Dacron , Kapton , Kevlar , Nomex , and Tedlar are registered trademarks of E.I. DuPont de Nemours & Co., Inc.

Duraback<sup>TM</sup> is a trademark of Unifax Corporation.

Durablanket is a registered trademark of Unifax Corporation.

Dyneema is a registered trademark of Toyobo Japan.

Fluorel<sup>TM</sup> is a trademark of Fluorel SA.

Kao-Tex<sup>TM</sup> is a trademark of Thermal Ceramics.

Microsoft is a registered trademark of Microsoft Corporation.

Nextel<sup>TM</sup> is a trademark of 3M Corporation.

Quartzel is a registered trademark of Saint-Gobain Industrial Ceramics.

Siltemp is a registered trademark of Amatek Chemical Products.

Solimide is a registered trademark of Inspec Foams.

Spectra is a registered trademark of Honeywell.

Superwool is a registered trademark of Morgan Materials Technology Ltd, England

Twaron is a registered trademark of Acordis.

Windows<sup>TM</sup> is a trademark of Microsoft Corporation.

Zetex and Zetex Plus are registered trademarks of Newtex Industries, Inc.

The findings in this report are not to be construed as an official Department of the Army position unless so designated by other authorized documents.

Citation of manufacturer's or trade names does not constitute an official endorsement or approval of the use thereof.

Destroy this report when it is no longer needed. Do not return it to the originator.